

Quantum-optical input-output relations for dispersive and lossy multilayer dielectric plates

T. Gruner and D.-G. Welsch

Friedrich-Schiller-Universität Jena, Theoretisch-Physikalisches Institut, Max-Wien-Platz 1, D-07743 Jena, Germany

(Received 28 November 1995; revised manuscript received 25 March 1996)

Using the Green-function approach to the problem of quantization of the phenomenological Maxwell theory, the propagation of quantized radiation through dispersive and absorptive multilayer dielectric plates is studied. Input-output relations are derived, with special emphasis on the determination of the quantum noise generators associated with the absorption of radiation inside the dielectric matter. The input-output relations are used to express arbitrary correlation functions of the outgoing field in terms of correlation functions of the incoming field and those of the noise generators. To illustrate the theory, photons at dielectric tunneling barriers are considered. It is shown that inclusion in the calculations of losses in the photonic band gaps may substantially change the barrier traversal times. [S1050-2947(96)02508-5]

PACS number(s): 42.50.Ct, 42.25.Bs, 42.79.-e, 73.40.Gk

I. INTRODUCTION

It is well known that the use of instruments in optical experiments needs careful examination with regard to their action on the quantum statistics of the light under study. In particular, the presence of passive instruments that may be regarded as macroscopic dielectric bodies responding linearly to radiation can be included in the theory by quantization of the phenomenological Maxwell theory for radiation in linear inhomogeneous dielectrics. The formalism was first developed for dispersionless and lossless dielectrics [1–4] and successfully applied to the study of the action of various devices, such as dielectric plates and interfaces [5,6] and optical cavities [7,8]. When broadband radiation propagates through dielectric devices the effects of dispersion and absorption, which are related to each other by the Kramers-Kronig relations, must necessarily be taken into account. In this context, a number of questions have arisen, such as the question about the velocity at which a single-photon wave packet travels in absorbing dielectric matter under the influence of normal and/or anomalous dispersion. Needless to say, absorption also introduces additional noise, at least the (quantum) vacuum noise.

The problem of describing the effects of dispersive and absorptive linear dielectric devices on quantized radiation has been considered in a number of papers and various quantization schemes have been proposed [9–17]. As we have recently shown, quantization of the radiation field within the framework of the phenomenological Maxwell theory (with given complex permittivity in the frequency domain) can be performed using a Green-function expansion of the operator of the vector potential [16,18]. This quantum-field-theoretical formalism, which may be regarded as a generalization of the familiar concepts of mode expansion, applies to both homogeneous and inhomogeneous dielectric matter and is consistent with both the Kramers-Kronig relations and the canonical (equal-time) field commutation relations in QED.

In the present paper we use the method in order to study the behavior of quantized radiation in the presence of multilayer dielectric plates and to derive input-output relations. The calculation of input-output relations is commonly based on a development of the familiar formalism of quan-

tum noise theory (see, e.g., [19]), in which the explicit nature of the input from a heat bath, and the output into it, is taken into account. The advantage of the quantum-field-theoretical approach is that it enables one to obtain the input-output relations including their dependence on frequency through geometry and dispersive and absorptive properties of the layers, because it consistently accounts for the effects of radiation-field propagation according to the (phenomenological) quantum Maxwell equations.

It is well known that when dielectric matter in free space is considered and the imaginary part of the permittivity may be disregarded (provided that the losses in the chosen frequency interval are sufficiently small), then the input-output relations correspond to unitary transformations between input- and output-mode operators [20,21]. These concepts fail when the effect of absorption of radiation through the dielectric matter is taken into account. In this case the outgoing fields are not only related to the incoming fields but also to appropriately chosen noise sources [22]. Neglect of these supplementary contributions would unavoidably lead to a violation of the canonical commutation relations for the outgoing fields, and hence effects of quantum noise would be left out.

Knowing the input-output relations, the properties of the outgoing fields can be obtained from those of the incoming fields and the dielectric-matter excitations. The multilayer dielectric structure under study may serve as a model for a number of devices, such as mirrors, beam splitters, interferometers, and optical fibers. In particular, multilayer dielectric mirrors may be regarded as tunnel barriers for photons [23] and can be used in order to measure barrier traversal times, as has recently been demonstrated in two-photon interference experiments [24–27]. In this context, we demonstrate the influence of losses in the photonic barriers on the apparently superluminal behavior of photons at such barriers and show that losses can substantially change the values of the traversal times.

The paper is organized as follows. In Sec. II the Green-function approach to the quantization of radiation in dispersive and lossy linear dielectrics is summarized. Applying the quantization scheme to radiation propagating through multilayer dielectric plates, in Sec. III input-output relations

are derived. In Sec. IV these relations are used to study normally ordered correlation functions of the outgoing fields, with special emphasis on the problem of photon tunneling through absorbing barriers. Finally, a summary and some conclusions are given in Sec. V.

II. QUANTIZATION SCHEME

A. Green-function approach

Let us consider linearly polarized radiation propagating in the x direction and allow for the presence of a multilayer dielectric plate characterized in terms of a frequency-dependent permittivity $\epsilon(x, \omega)$ that varies in x direction and obeys, for causality reasons, the Kramers-Kronig relations. Introducing the vector potential $A(x, t)$ and using the relation

$$D(x, t) = \epsilon_0 \left[E(x, t) + \int_{-\infty}^t d\tau \chi(t - \tau) E(x, \tau) \right] \quad (1)$$

($E = -\dot{A}$), the classical phenomenological Maxwell equations yield

$$\frac{\partial^2}{\partial x^2} A(x, t) - \frac{1}{c^2} \left[\ddot{A}(x, t) + \int_{-\infty}^t d\tau \chi(t - \tau) \ddot{A}(x, \tau) \right] = 0, \quad (2)$$

which in the frequency domain reads as

$$\left[\frac{\partial^2}{\partial x^2} + \frac{\omega^2}{c^2} \epsilon(x, \omega) \right] A(x, \omega) = 0. \quad (3)$$

Equation (3) may be transferred to quantum theory as follows [16,18]:

$$\left[\frac{\partial^2}{\partial x^2} + \frac{\omega^2}{c^2} \epsilon(x, \omega) \right] \hat{A}(x, \omega) = \hat{j}(x, \omega), \quad (4)$$

where the ‘‘current’’ operator

$$\hat{j}(x, \omega) = \frac{\omega}{c^2} \sqrt{\frac{\hbar}{\pi \epsilon_0 \mathcal{A}}} \epsilon_i(x, \omega) \hat{f}(x, \omega) \quad (5)$$

is introduced to take into account the noise owing to absorption. In Eq. (5), $\hat{f}(x, \omega)$ and $\hat{f}^\dagger(x, \omega)$ are bosonic field operators,

$$[\hat{f}(x, \omega), \hat{f}^\dagger(x', \omega')] = \delta(x - x') \delta(\omega - \omega'), \quad (6)$$

$$[\hat{f}(x, \omega), \hat{f}(x', \omega')] = [\hat{f}^\dagger(x, \omega), \hat{f}^\dagger(x', \omega')] = 0, \quad (7)$$

and

$$\epsilon(x, \omega) = \epsilon_r(x, \omega) + i \epsilon_i(x, \omega) \quad (8)$$

(\mathcal{A} , normalization area in the yz plane). The solution of Eq. (4) may be given by

$$\hat{A}(x, \omega) = \int dx' G(x, x', \omega) \hat{j}(x', \omega), \quad (9)$$

where $G(x, x', \omega)$ is the classical Green function obeying the equation

$$\left[\frac{\partial^2}{\partial x^2} + \frac{\omega^2}{c^2} \epsilon(x, \omega) \right] G(x, x', \omega) = \delta(x - x') \quad (10)$$

and tending to zero as $x \rightarrow \pm \infty$. It can be shown [16,18] that the quantization scheme outlined above ensures that the (Schrödinger) operators of the vector potential and the electric-field strength,

$$\hat{A}(x) = \int_0^\infty d\omega \hat{A}(x, \omega) + \text{H.c.}, \quad (11)$$

$$\hat{E}(x) = i \int_0^\infty d\omega \omega \hat{A}(x, \omega) + \text{H.c.}, \quad (12)$$

satisfy the well-known canonical commutation relation

$$[\hat{A}(x), \hat{E}(x')] = -\frac{i\hbar}{\mathcal{A}\epsilon_0} \delta(x - x'). \quad (13)$$

B. Quantum Langevin equations

From Eqs. (11), (9), and (10) we see that the problem of determining the operator of the vector potential reduces to the calculation of the classical Green function. Before performing the calculations for multilayer dielectric plates, let us summarize some results for homogeneous dielectrics, where

$$\begin{aligned} G(x, x', \omega) &= \frac{1}{2\pi} \int_{-\infty}^\infty dk e^{ik(x-x')} \frac{c^2}{\omega^2 \epsilon(\omega) - c^2 k^2} \\ &= \left[2i \frac{\omega}{c} n(\omega) \right]^{-1} \exp \left[i \frac{\omega}{c} n(\omega) |x - x'| \right]. \end{aligned} \quad (14)$$

Here

$$n(\omega) = \sqrt{\epsilon(\omega)} = \beta(\omega) + i\gamma(\omega) \quad (15)$$

is the complex refractive index. Using Eqs. (9) and (14), Eq. (11) may be rewritten as

$$\begin{aligned} \hat{A}(x) &= \int_0^\infty d\omega \sqrt{\frac{\hbar}{4\pi c \omega \epsilon_0 \beta(\omega) \mathcal{A} n(\omega)}} \\ &\quad \times [e^{i\beta(\omega)\omega x/c} \hat{a}_+(x, \omega) \\ &\quad + e^{-i\beta(\omega)\omega x/c} \hat{a}_-(x, \omega)] + \text{H.c.}, \end{aligned} \quad (16)$$

where the operators

$$\begin{aligned} \hat{a}_\pm(x, \omega) &= \frac{1}{i} \sqrt{2\gamma(\omega) \frac{\omega}{c}} e^{\mp \gamma(\omega)\omega x/c} \\ &\quad \times \int_{-\infty}^{\pm x} dx' e^{-in(\omega)\omega x'/c} \hat{f}(\pm x', \omega) \end{aligned} \quad (17)$$

associated with the waves propagating to the right (+) and left (−) are introduced. In the limiting case when the absorption may be disregarded [$\gamma(\omega)\omega|x - x'|/c \rightarrow 0$], Eq. (16) reduces to the familiar mode-expansion result [16,18]. In particular, the operators $\hat{a}_\pm(x, \omega)$ and $\hat{a}_\pm^\dagger(x, \omega)$ become

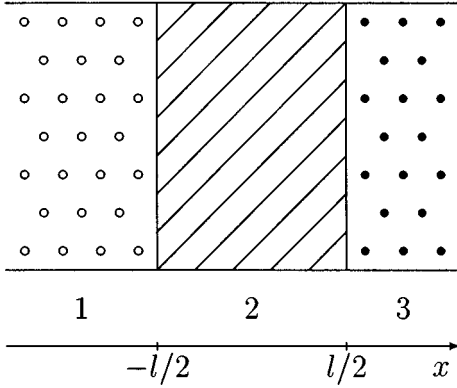


FIG. 1. Scheme of the single-slab dielectric plate (2) of thickness l embedded in dielectric matter (1 and 3).

independent of x and satisfy the well-known commutation relations for photon destruction and creation operators, respectively.

Equation (17) implies that the operators $\hat{a}_{\pm}(x, \omega)$ and $\hat{a}_{\pm}(x', \omega)$ can be related to each other as

$$\hat{a}_{\pm}(x, \omega) = \hat{a}_{\pm}(x', \omega) e^{\mp \gamma(\omega)\omega(x-x')/c} + \int_{x'}^x dy \hat{F}_{\pm}(y, \omega) e^{\mp \gamma(\omega)\omega(x-y)/c}, \quad (18)$$

where

$$\hat{F}_{\pm}(x, \omega) = \pm \frac{1}{i} \sqrt{2\gamma(\omega)\frac{\omega}{c}} e^{\mp i\beta(\omega)\omega x/c} \hat{f}_{\pm}(x, \omega). \quad (19)$$

Hence the operators $\hat{a}_{\pm}(x, \omega)$ obey quantum Langevin equations in the space domain [18],

$$\frac{\partial}{\partial x} \hat{a}_{\pm}(x, \omega) = \mp \gamma(\omega) \frac{\omega}{c} \hat{a}_{\pm}(x, \omega) + \hat{F}_{\pm}(x, \omega), \quad (20)$$

where the operators $\hat{F}_{\pm}(x, \omega)$ may be regarded as Langevin noise sources,

$$[\hat{F}_{\pm}(x, \omega), \hat{F}_{\pm}^{\dagger}(x', \omega')] = 2\gamma(\omega) \frac{\omega}{c} \delta(x-x') \delta(\omega-\omega'), \quad (21)$$

$$[\hat{F}_{\pm}(x, \omega), \hat{a}_{\pm}^{\dagger}(x', \omega')] = \pm \Theta(\pm x' \mp x) 2\gamma(\omega) \frac{\omega}{c} \times e^{-\gamma(\omega)\omega|x'-x|/c} \delta(\omega-\omega'). \quad (22)$$

III. INPUT-OUTPUT RELATIONS

We now turn to the problem of propagation of quantized radiation through multilayer dielectric plates. Assuming N dielectric slabs, the interfaces being parallel to the yz plane (cf. Figs. 1 and 2), the permittivity may be given by

$$\epsilon(x, \omega) = \sum_{j=1}^N \lambda_j(x) \epsilon_j(\omega), \quad (23)$$

where

$$\lambda_j(x) = \begin{cases} 1 & \text{if } x_{j-1} < x < x_j \\ 0 & \text{otherwise} \end{cases} \quad (24)$$

is the characteristic function of the j th slab ($x_0 \rightarrow -\infty$, $x_N \rightarrow \infty$). In particular, for $N \geq 3$ the system represents an $(N-2)$ -slab dielectric plate surrounded by dielectric matter whose permittivity on the left and right, respectively, is $\epsilon_1(\omega)$ and $\epsilon_N(\omega)$. To determine the Green function $G(x, x', \omega)$ that satisfies Eq. (10) (and vanishes at infinity), we note that $G(x, x', \omega)$ can be decomposed into two parts,

$$G(x, x', \omega) = G_0(x, x', \omega) + G_1(x, x', \omega), \quad (25)$$

where, according to Eq. (14),

$$G_0(x, x', \omega) = \sum_{j=1}^N \lambda_j(x) \lambda_j(x') \left[2i \frac{\omega}{c} n_j(\omega) \right]^{-1} \times \exp \left[i \frac{\omega}{c} n_j(\omega) |x-x'| \right], \quad (26)$$

and $G_1(x, x', \omega)$ is the solution of the homogeneous equation

$$\left[\frac{\partial^2}{\partial x^2} + \frac{\omega^2}{c^2} \epsilon(x, \omega) \right] G_1(x, x', \omega) = 0, \quad (27)$$

which implies that

$$G_1(x, x', \omega) = \sum_{j=1}^N \lambda_j(x) [C_j^{(1)}(x', \omega) e^{in_j(\omega)\omega x/c} + C_j^{(2)}(x', \omega) e^{-in_j(\omega)\omega x/c}]. \quad (28)$$

Clearly, the $C_j^{(1)}(x', \omega)$ and $C_j^{(2)}(x', \omega)$ must be determined in such a way that $G(x, x', \omega)$ vanishes at infinity and is continuously differentiable at the surfaces of discontinuity. The somewhat lengthy calculations may be performed in a straightforward way. For the simplest case of a single-slab dielectric plate embedded in dielectric matter ($N=3$, cf. Fig. 1), the result is given in Appendix A. Because of the voluminous formulas, we renounce their presentation for the general case.

Combining Eqs. (9) and (25) [together with Eqs. (26) and (28)], the (Schrödinger) operator of the vector potential $\hat{A}(x)$ for the j th domain ($j=1, \dots, N$) may be represented as, similar to Eq. (16),

$$\hat{A}(x) = \int_0^{\infty} d\omega \sqrt{\frac{\hbar}{4\pi c \omega \epsilon_0 \beta_j(\omega) \mathcal{A} n_j(\omega)}} \times [e^{i\beta_j(\omega)\omega x/c} \hat{a}_{j+}(x, \omega) + e^{-i\beta_j(\omega)\omega x/c} \hat{a}_{j-}(x, \omega)] + \text{H.c.} \quad (29)$$

($x_{j-1} \leq x \leq x_j$), where the dependence on x of the amplitude operators $\hat{a}_{j\pm}(x, \omega)$ is governed by quantum Langevin equations of the type given in Eq. (20) together with Eqs. (19)

and (21) $[\beta(\omega), \gamma(\omega) \rightarrow \beta_j(\omega), \gamma_j(\omega)]$, so that $\hat{a}_{j\pm}(x, \omega)$ can be represented in the form (18), viz.,

$$\hat{a}_{j\pm}(x, \omega) = \hat{a}_{j\pm}(x', \omega) e^{\mp \gamma_j(\omega)\omega(x-x')/c} + \int_{x'}^x dy \hat{F}_{j\pm}(y, \omega) e^{\mp \gamma_j(\omega)\omega(x-y)/c} \quad (30)$$

($x_{j-1} \leq x, x' \leq x_j$), where

$$\hat{F}_{j\pm}(x, \omega) = \pm \frac{1}{i} \sqrt{2\gamma_j(\omega)} \frac{\omega}{c} e^{\mp i\beta_j(\omega)\omega x/c} \hat{f}(x, \omega). \quad (31)$$

Since the relations between $\hat{a}_{j\pm}(x, \omega)$ and $\hat{f}(x, \omega)$ sensitively depend on the actual expression for $G(x, x', \omega)$, the commutation relations (22) [that are based on Eq. (17)] cannot be applied in general. Successive application of Eq. (30) enables one to relate the (amplitude) operators $\hat{a}_{1-}(x, \omega)$ ($-\infty \leq x \leq x_1$) and $\hat{a}_{N+}(x, \omega)$ ($x_{N-1} \leq x \leq \infty$) for the outgoing fields to the left and right, respectively, to the operators of the corresponding incoming fields, $\hat{a}_{1+}(x, \omega)$ and $\hat{a}_{N-}(x, \omega)$, and operator noise sources associated with the losses owing to absorption.

A. Single-slab dielectric plate

To illustrate the procedure outlined, let us first study the input-output relations for a single-slab dielectric plate of thickness l embedded in two (different) dielectrics ($N=3$, cf. Fig. 1). Substituting in Eq. (9) for $G(x, x', \omega)$ the expression (A1) given in Appendix A and introducing the (amplitude) operators $\hat{a}_{1\pm}(x, \omega)$, $-\infty \leq x \leq -l/2$, and $\hat{a}_{3\pm}(x, \omega)$, $l/2 \leq x \leq \infty$ [Appendix B 1, Eqs. (B1)–(B4)], the input operators are found to satisfy the commutation relations

$$[\hat{a}_{1+}(x, \omega), \hat{a}_{1+}^\dagger(x', \omega')] = e^{-\gamma_1(\omega)\omega|x-x'|/c} \delta(\omega - \omega'), \quad (32)$$

$$[\hat{a}_{3-}(x, \omega), \hat{a}_{3-}^\dagger(x', \omega')] = e^{-\gamma_3(\omega)\omega|x-x'|/c} \delta(\omega - \omega'), \quad (33)$$

$$[\hat{a}_{1+}(x, \omega), \hat{a}_{3-}^\dagger(x', \omega')] = 0 \quad (34)$$

[Eqs. (B20)–(B22)], so that the input fields from the left and right behave like the fields in the corresponding bulk dielectrics and may be regarded as independent variables. Note that $\hat{a}_{1+}(x, \omega), \hat{a}_{3-}(x, \omega)$ are commuting quantities.

Defining operators

$$\hat{g}_\pm^{(1)}(\omega) = [2c_\pm(l, \omega)]^{-1/2} [\hat{g}'_-(\omega) \pm \hat{g}'_+(\omega)], \quad (35)$$

where

$$\hat{g}'_\pm(\omega) = \frac{1}{i} \sqrt{\frac{\omega}{c}} e^{in_2(\omega)\omega l/(2c)} \int_{-l/2}^{l/2} dx' e^{\mp in_2(\omega)\omega x'/c} \hat{f}(x', \omega) \quad (36)$$

and

$$c_\pm(l, \omega) = e^{-\gamma_2(\omega)\omega l/c} \frac{1}{\gamma_2(\omega)} \sinh\left[\gamma_2(\omega) \frac{\omega}{c} l\right] \pm e^{-\gamma_2(\omega)\omega l/c} \frac{1}{\beta_2(\omega)} \sin\left[\beta_2(\omega) \frac{\omega}{c} l\right], \quad (37)$$

and recalling Eqs. (6) and (7), we find that

$$[\hat{g}_\pm^{(1)}(\omega), (\hat{g}_\pm^{(1)}(\omega'))^\dagger] = \delta(\omega - \omega'), \quad (38)$$

$$[\hat{g}_\pm^{(1)}(\omega), (\hat{g}_\mp^{(1)}(\omega'))^\dagger] = 0. \quad (39)$$

Since

$$\begin{aligned} [\hat{a}_{1+}(x, \omega), (\hat{g}_\pm^{(1)}(\omega'))^\dagger] &= 0 \\ &= [\hat{a}_{3-}(x, \omega), (\hat{g}_\pm^{(1)}(\omega'))^\dagger] \end{aligned} \quad (40)$$

[Eq. (B23)], the incoming-field (amplitude) operators and the operators $\hat{g}_\pm^{(1)}(\omega), (\hat{g}_\pm^{(1)})^\dagger(\omega)$ may be regarded as being independent variables (note that $\hat{a}_{1+}, \hat{a}_{3-}$, and $\hat{g}_\pm^{(1)}$ commute). Moreover, the $\hat{g}_\pm^{(1)}(\omega)$ and $(\hat{g}_\pm^{(1)})^\dagger(\omega)$, respectively, which are obviously destruction and creation operators of bosonic excitations associated with the plate, play the role of the additional operator noise sources in the input-output relations

$$\begin{pmatrix} \hat{a}_{1-}(-\frac{1}{2}l, \omega) \\ \hat{a}_{3+}(\frac{1}{2}l, \omega) \end{pmatrix} = \tilde{\mathbf{T}}^{(1)} \begin{pmatrix} \hat{a}_{1+}(-\frac{1}{2}l, \omega) \\ \hat{a}_{3-}(\frac{1}{2}l, \omega) \end{pmatrix} + \tilde{\mathbf{A}}^{(1)} \begin{pmatrix} \hat{g}_+^{(1)}(\omega) \\ \hat{g}_-^{(1)}(\omega) \end{pmatrix} \quad (41)$$

derived in Appendix B1 [Eq. (B5)], the elements of the 2×2 matrices

$$\tilde{\mathbf{T}}^{(1)} = \begin{pmatrix} T_{11}^{(1)}(\omega) & T_{12}^{(1)}(\omega) \\ T_{21}^{(1)}(\omega) & T_{22}^{(1)}(\omega) \end{pmatrix} \quad (42)$$

and

$$\tilde{\mathbf{A}}^{(1)} = \begin{pmatrix} A_{11}^{(1)}(\omega) & A_{12}^{(1)}(\omega) \\ A_{21}^{(1)}(\omega) & A_{22}^{(1)}(\omega) \end{pmatrix} \quad (43)$$

being given in Eqs. (B6)–(B13) [note the simplifications (B14)–(B19) when the plate is surrounded by vacuum]. In Eq. (41) the (amplitude) operators of the outgoing fields, $\hat{a}_{1-}(-l/2, \omega)$ and $\hat{a}_{3+}(l/2, \omega)$, are expressed in terms of the operators of the incoming fields, $\hat{a}_{1+}(-l/2, \omega)$ and $\hat{a}_{3-}(l/2, \omega)$, and the operator noise sources $\hat{g}_\pm^{(1)}(\omega)$. The characteristic transformation matrix of the plate, $\tilde{\mathbf{T}}^{(1)}$, which for an approximately lossless dielectric plate in free space reduces to the well-known characteristic matrix given, e.g., in [28], describes the effects of transmission and reflection of the input fields, whereas the losses inside the plate give rise to an additional matrix, $\tilde{\mathbf{A}}^{(1)}$, which may be called the characteristic absorption matrix.

It should be mentioned that the output amplitude operators $\hat{a}_{1-}(x)$, $x \leq -l/2$, and $\hat{a}_{3+}(x)$, $x \geq l/2$, can easily be obtained from Eq. (30), with $x' = -l/2$ and $x' = l/2$, respectively, and application of the input-output relations (41). The resulting representation of the outgoing fields is of course

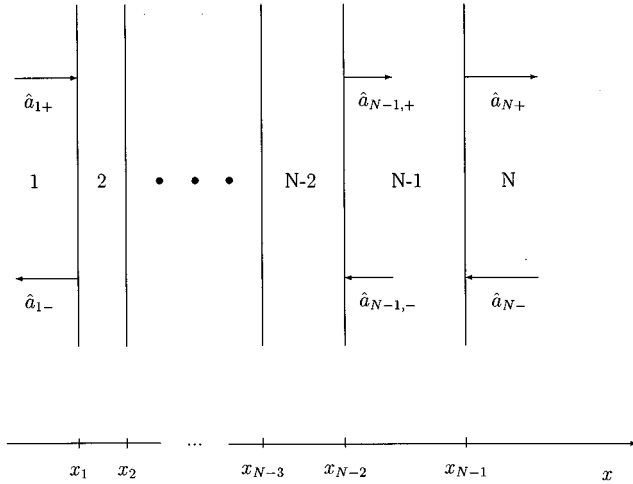


FIG. 2. Scheme of the multilayer dielectric configuration, the arrows together with the amplitude operators indicating incoming and outgoing fields.

fully equivalent to the Green's function expansion primarily used. The commutation relations for the output amplitude operators are given in Appendix B1 [Eqs. (B24)–(B26)]. They differ, in general, from those given in Eqs. (32)–(34) for the input operators. The differences vanish when the distances from the plate are large compared with the (classical) absorption length or when the plate is in free space.

B. Multilayer dielectric plates

The results given in Sec. III A can be extended to an arbitrary multilab dielectric structure ($N \geq 3$, cf. Fig. 2) in a straightforward way (for details see Appendix B 2). In particular, the input-output relations may be given by

$$\begin{pmatrix} \hat{a}_{1-}(x_1, \omega) \\ \hat{a}_{N+}(x_{N-1}, \omega) \end{pmatrix} = \tilde{\mathbf{T}}^{(N-2)} \begin{pmatrix} \hat{a}_{1+}(x_1, \omega) \\ \hat{a}_{N-}(x_{N-1}, \omega) \end{pmatrix} + \tilde{\mathbf{A}}^{(N-2)} \begin{pmatrix} \hat{g}_+^{(N-2)}(\omega) \\ \hat{g}_-^{(N-2)}(\omega) \end{pmatrix}. \quad (44)$$

Here, $x = x_1$ and $x = x_{N-1}$, respectively, are the left and right surfaces of the multilab plate (note that for the single-slab plate, $N = 3$, the notations $x_1 = -l/2$ and $x_{N-1} = x_2 = l/2$ have been used). The commutation rules for the input operators $\hat{a}_{1+}(x, \omega)$, $\hat{a}_{1+}^\dagger(x, \omega)$ ($-\infty \leq x \leq x_1$), $\hat{a}_{N-}(x, \omega)$, $\hat{a}_{N-}^\dagger(x, \omega)$ ($x_{N-1} \leq x \leq \infty$), and the noise operators $\hat{g}_\pm^{(N-2)}(\omega)$ are the same as in the preceding section, i.e.,

$$[\hat{a}_{1+}(x, \omega), \hat{a}_{1+}^\dagger(x', \omega')] = e^{-\gamma_1(\omega)} \omega^{|x-x'|/c} \delta(\omega - \omega'), \quad (45)$$

$$[\hat{a}_{N-}(x, \omega), \hat{a}_{N-}^\dagger(x', \omega')] = e^{-\gamma_N(\omega)} \omega^{|x-x'|/c} \delta(\omega - \omega'), \quad (46)$$

$$[\hat{a}_{1+}(x, \omega), \hat{a}_{N-}^\dagger(x', \omega')] = 0, \quad (47)$$

$$[\hat{g}_\pm^{(N-2)}(\omega), (\hat{g}_\pm^{(N-2)}(\omega'))^\dagger] = \delta(\omega - \omega'), \quad (48)$$

$$[\hat{g}_\pm^{(N-2)}(\omega), (\hat{g}_\mp^{(N-2)}(\omega'))^\dagger] = 0, \quad (49)$$

$$\begin{aligned} [\hat{a}_{1+}(x, \omega), (\hat{g}_\pm^{(N-2)}(\omega'))^\dagger] &= 0 \\ &= [\hat{a}_{N-}(x, \omega), (\hat{g}_\pm^{(N-2)}(\omega'))^\dagger]. \end{aligned} \quad (50)$$

The input-output relations (44) [together with the commutation relations (45)–(50)] apply to arbitrary multilab dielectric equipment described in terms of a complex permittivity that spatially varies as a multistep function and whose dependence on frequency is consistent with the Kramers-Kronig relations over the whole frequency domain. Typical examples are fractionally transparent dielectric mirrors and combinations of them, such as resonatorlike cavities bounded by dielectric walls. In particular, when the overall device is surrounded by vacuum, so that the incoming and outgoing radiation fields propagate in free space,

$$n_1(\omega) = n_N(\omega) \equiv 1, \quad (51)$$

the familiar mode expansions for the input and output (free) fields are recognized. For $j = 1, N$ Eq. (29) takes the form

$$\begin{aligned} \hat{A}(x) &= \int_0^\infty d\omega \sqrt{\frac{\hbar}{4\pi c \omega \epsilon_0 \mathcal{A}}} \\ &\times [e^{i\omega x/c} \hat{a}_{j+}(\omega) + e^{-i\omega x/c} \hat{a}_{j-}(\omega)] + \text{H.c.}, \end{aligned} \quad (52)$$

where the input and output operators $\hat{a}_{1\pm}(\omega)$ [$\hat{a}_{1\pm}^\dagger(\omega)$] and $\hat{a}_{N\pm}(\omega)$ [$\hat{a}_{N\pm}^\dagger(\omega)$], respectively, are proper (space-independent) photon destruction (creation) operators, and

$$\begin{pmatrix} \hat{a}_{1-}(\omega) \\ \hat{a}_{N+}(\omega) \end{pmatrix} = \tilde{\mathbf{T}}^{(N-2)} \begin{pmatrix} \hat{a}_{1+}(\omega) \\ \hat{a}_{N-}(\omega) \end{pmatrix} + \tilde{\mathbf{A}}^{(N-2)} \begin{pmatrix} \hat{g}_+^{(N-2)}(\omega) \\ \hat{g}_-^{(N-2)}(\omega) \end{pmatrix}. \quad (53)$$

The influence of the plate on the incident light through reflection and transmission from the two sides is described by the matrix elements $T_{ik}^{(N-2)}(\omega)$, whereas the matrix elements $A_{ik}^{(N-2)}(\omega)$ arise from absorption. From Eqs. (45)–(47), the bosonic commutation relations for the input-mode operators $\hat{a}_{1+}(\omega)$, $\hat{a}_{N-}(\omega)$ are easily seen to be satisfied. Using them and recalling the commutation rules (48)–(50), the bosonic commutation relations for the output-mode operators $\hat{a}_{1-}(\omega)$, $\hat{a}_{N+}(\omega)$ can then be obtained by means of the input-output relations (53), because the relations

$$\begin{aligned} |T_{11}^{(N-2)}|^2 + |T_{12}^{(N-2)}|^2 + |A_{11}^{(N-2)}|^2 + |A_{12}^{(N-2)}|^2 \\ = |T_{21}^{(N-2)}|^2 + |T_{22}^{(N-2)}|^2 + |A_{21}^{(N-2)}|^2 + |A_{22}^{(N-2)}|^2 = 1 \end{aligned} \quad (54)$$

and

$$\begin{aligned} T_{11}^{(N-2)}(T_{21}^{(N-2)})^* + T_{12}^{(N-2)}(T_{22}^{(N-2)})^* + A_{11}^{(N-2)}(A_{21}^{(N-2)})^* \\ + A_{12}^{(N-2)}(A_{22}^{(N-2)})^* = 0 \end{aligned} \quad (55)$$

are valid [see Appendixes B 1 and B 2]. For notational convenience, the frequency arguments of the matrix elements

$T_{ik}^{(N-2)}$ and $A_{ik}^{(N-2)}$ are omitted. In particular, these relations reflect the fact that the sum of the probabilities for reflection, transmission, and absorption of a photon is equal to unity. If the losses inside the plate can approximately be disregarded, $\tilde{\mathbf{A}}^{(N-2)} \approx 0$, the well-known method of unitary transformation is recognized. In this case the relations (54) and (55) simplify to

$$|T_{11}^{(N-2)}|^2 + |T_{12}^{(N-2)}|^2 = |T_{21}^{(N-2)}|^2 + |T_{22}^{(N-2)}|^2 = 1, \quad (56)$$

$$T_{11}^{(N-2)}(T_{21}^{(N-2)})^* + T_{12}^{(N-2)}(T_{22}^{(N-2)})^* = 0, \quad (57)$$

so that $\tilde{\mathbf{T}}^{(N-2)}$ becomes a unitary matrix. Since the photon operators of the output and input modes are uniquely related to each other through a unitary transformation, the bosonic commutation relations are automatically preserved. In general, the $\tilde{\mathbf{T}}^{(N-2)}$ matrix is not unitary and the output-mode operators are obtained, according to Eq. (53), from both the input-mode operators and the noise operators associated with the losses. The relations (54) and (55), which are the natural generalization of the relations (56) and (57), may be regarded as necessary conditions imposed on the $\tilde{\mathbf{T}}^{(N-2)}$ and $\tilde{\mathbf{A}}^{(N-2)}$ matrices of an arbitrary dispersive and absorptive multilayer dielectric device in free space. It should be emphasized that these conditions need not be postulated, but they necessarily come out of the theory, which also enables one to systematically calculate both the $\tilde{\mathbf{T}}^{(N-2)}$ and $\tilde{\mathbf{A}}^{(N-2)}$ matrices.

IV. APPLICATIONS

A. Radiation-field correlation functions

The input-output relations (53) can be used to obtain the quantum statistical properties of the outgoing radiation from the properties of the incoming radiation and the excitations associated with the dielectric matter. With regard to measurement, the quantum statistics of radiation is frequently described in terms of normally ordered correlation functions, such as correlation functions of the electric-field strength or

the photon creation and destruction operators (see, e.g., [4,30]). Introducing the notations $\hat{a}_1 \equiv \hat{a}_{1+}$, $\hat{a}_2 \equiv \hat{a}_{N-}$, $\hat{a}'_1 \equiv \hat{a}_{1-}$, $\hat{a}'_2 \equiv \hat{a}_{N+}$ and $\hat{g}_1 \equiv \hat{g}_+^{(N-2)}$, $\hat{g}_2 \equiv \hat{g}_-^{(N-2)}$, from Eqs. (12) and (52), the electric-field strength of the outgoing radiation in the i th channel ($i=1,2$) reads as

$$\hat{E}'_i(x) = \hat{E}'_i^{(+)}(x) + \hat{E}'_i^{(-)}(x), \quad (58)$$

$$\hat{E}'_i^{(+)}(x) = i \int_0^\infty d\omega \sqrt{\frac{\hbar \omega}{4\pi c \epsilon_0 \mathcal{A}}} e^{i\omega \eta_i x/c} \hat{a}'_i(\omega), \quad (59)$$

$$\hat{E}'_i^{(-)}(x) = [\hat{E}'_i^{(+)}(x)]^\dagger \quad (60)$$

($\eta_1=1$, $\eta_2=-1$), where the output-photon operators $\hat{a}'_i(\omega)$ can be related to the input-photon operators $\hat{a}_i(\omega)$ as, according to Eq. (53),

$$\hat{a}'_i(\omega) = \sum_{k=1}^2 [T_{ik}(\omega) \hat{a}_k(\omega) + A_{ik}(\omega) \hat{g}_k(\omega)] \quad (61)$$

[$T_{ik}(\omega) \equiv T_{ik}^{(N-2)}(\omega)$, $A_{ik}(\omega) \equiv A_{ik}^{(N-2)}(\omega)$]. To express the normally ordered electric-field correlation functions of the outgoing radiation,

$$C'^{(m,n)}_{\{i_\mu\}}(\{x_\mu, t_\mu\}) = \left\langle \left[\prod_{\mu=1}^m \hat{E}'_{i_\mu}{}^{(-)}(x_\mu, t_\mu) \right] \times \left[\prod_{\mu=m+1}^{m+n} \hat{E}'_{i_\mu}{}^{(+)}(x_\mu, t_\mu) \right] \right\rangle, \quad (62)$$

in terms of normally ordered correlation functions of photon creation and destruction operators, we use Eqs. (58)–(60) and recall the harmonic (exponential) time evolution of the photon destruction operators in the Heisenberg picture. We obtain

$$C'^{(m,n)}_{\{i_\mu\}}(\{x_\mu, t_\mu\}) = i^{n-m} \left(\frac{\hbar}{4\pi c \epsilon_0 \mathcal{A}} \right)^{(n+m)/2} \int_0^\infty d\omega_1 \sqrt{\omega_1} e^{i\omega_1 \tau_1} \dots \int_0^\infty d\omega_{m+n} \sqrt{\omega_{m+n}} e^{-i\omega_{m+n} \tau_{m+n}} \underline{C}'_{\{i_\mu\}}{}^{(m,n)}(\{\omega_\mu\}) \quad (63)$$

($\tau_{i_\mu} = t_\mu - \eta_{i_\mu} x_\mu / c$), where

$$\underline{C}'_{\{i_\mu\}}{}^{(m,n)}(\{\omega_\mu\}) = \left\langle \left[\prod_{\mu=1}^m \hat{a}'_{i_\mu}{}^\dagger(\omega_\mu) \right] \left[\prod_{\mu=m+1}^{m+n} \hat{a}'_{i_\mu}(\omega_\mu) \right] \right\rangle, \quad (64)$$

which can be rewritten as, on using the input-output relations (61),

$$\underline{C}'_{\{i_\mu\}}{}^{(m,n)}(\{\omega_\mu\}) = \left\langle \left\{ \prod_{\mu=1}^m \sum_{k_\mu=1}^2 [T_{i_\mu k_\mu}^*(\omega_\mu) \hat{a}_{k_\mu}^\dagger(\omega_\mu) + A_{i_\mu k_\mu}^*(\omega_\mu) \hat{g}_{k_\mu}^\dagger(\omega_\mu)] \right\} \times \left\{ \prod_{\mu=m+1}^{m+n} \sum_{k_\mu=1}^2 [T_{i_\mu k_\mu}(\omega_\mu) \hat{a}_{k_\mu}(\omega_\mu) + A_{i_\mu k_\mu}(\omega_\mu) \hat{g}_{k_\mu}(\omega_\mu)] \right\} \right\rangle. \quad (65)$$

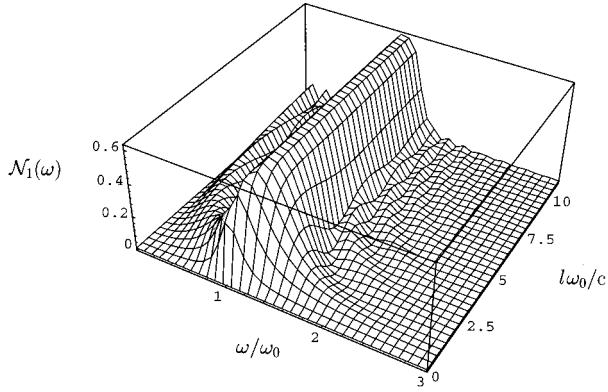


FIG. 3. The ratio of the photon-number densities of the reflected outgoing field and the incoming field, $\mathcal{N}_1(\omega) = N'_{\text{ph}1}(\omega) / N_{\text{ph}1}(\omega)$, as a function of frequency and plate thickness for a single-resonance medium ($\omega_0 = \omega_1$, $\Gamma = 0.1\omega_0$).

In particular, when the states of the incoming radiation and the dielectric matter are not correlated to each other, the correlation functions of the output photons, Eq. (65), can be expressed in terms of sums of products of input-photon correlation functions

$$\underline{C}_{\{i_\mu\}}^{(k,l)}(\{\omega_\mu\}) = \left\langle \left[\prod_{\mu=1}^k \hat{a}_{i_\mu}^\dagger(\omega_\mu) \right] \left[\prod_{\mu=l+1}^{k+l} \hat{a}_{i_\mu}(\omega_\mu) \right] \right\rangle \quad (66)$$

and correlation functions of the excitations associated with the dielectric matter,

$$\underline{\Gamma}_{\{i_\mu\}}^{(p,q)}(\{\omega_\mu\}) = \left\langle \left[\prod_{\mu=1}^p \hat{g}_{i_\mu}^\dagger(\omega_\mu) \right] \left[\prod_{\mu=p+1}^{p+q} \hat{g}_{i_\mu}(\omega_\mu) \right] \right\rangle, \quad (67)$$

with $k, p \leq m$ and $l, q \leq n$. Clearly, when the matter is prepared in an incoherent state, then the correlation functions $\underline{\Gamma}_{\{i_\mu\}}^{(p,q)}(\{\omega_\mu\})$ vanish when $p \neq q$ (explicit expressions for the correlation functions observed when the matter is thermally excited are given in Appendix C).

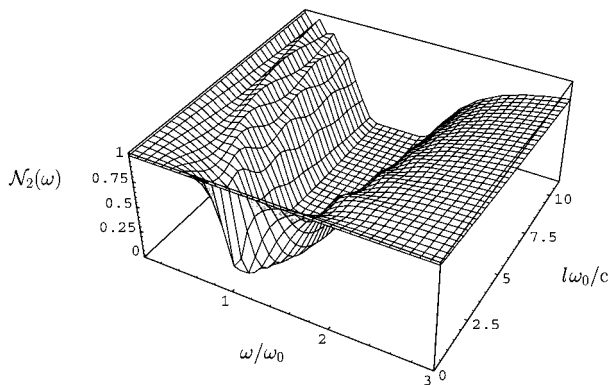


FIG. 4. The ratio of the photon-number densities of the transmitted outgoing field and the incoming field, $\mathcal{N}_2(\omega) = N'_{\text{ph}2}(\omega) / N_{\text{ph}1}(\omega)$, as a function of frequency and plate thickness for a single-resonance medium ($\omega_0 = \omega_1$, $\Gamma = 0.1\omega_0$).

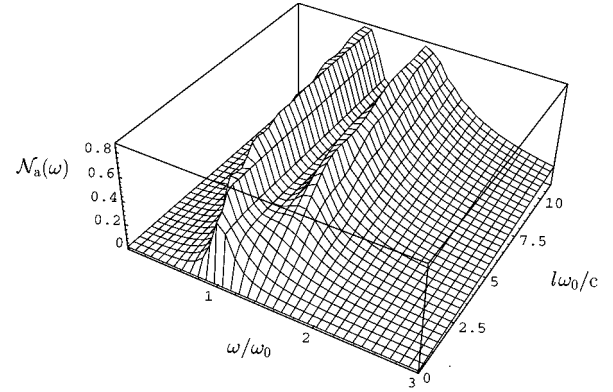


FIG. 5. The ratio of the photon-number densities of the absorbed field and the incoming field, $\mathcal{N}_a = \{N_{\text{ph}1}(\omega) - [N'_{\text{ph}1}(\omega) + N'_{\text{ph}2}(\omega)]\} / N_{\text{ph}1}(\omega) = \alpha_1(\omega) = \alpha_2(\omega)$, as a function of frequency and plate thickness for a single-resonance medium ($\omega_0 = \omega_1$, $\Gamma = 0.1\omega_0$).

B. Spectral photon-number densities

Let us briefly consider the photon-number density (number of photons per unit frequency) in the i th output channel ($i = 1, 2$),

$$N'_{\text{ph}i}(\omega) = \langle \hat{a}'_i^\dagger(\omega) \hat{a}'_i(\omega) \rangle = C'^{(1,1)}_i(\omega, \omega), \quad (68)$$

which can easily be obtained from application of Eqs. (65)–(67). In particular, when a zero-temperature dielectric plate is irradiated from one side [$N_{\text{ph}2}(\omega) = 0$] we find that

$$N'_{\text{ph}i}(\omega) = |T_{i1}(\omega)|^2 N_{\text{ph}1}(\omega) \quad (i = 1, 2). \quad (69)$$

As expected, the mean photon-number densities in the output channels 1 and 2, respectively, are simply given by the mean input photon-number density multiplied by the reflection and transmission coefficients. In general, the overall output photon-number density is reduced below the input level owing to absorption:

$$N'_{\text{ph}1}(\omega) + N'_{\text{ph}2}(\omega) \leq N_{\text{ph}1}(\omega). \quad (70)$$

In Figs. 3 and 4 the relative photon-number densities of the outgoing radiation, $\mathcal{N}_1 \equiv N'_{\text{ph}1}(\omega) / N_{\text{ph}1}(\omega) = |T_{11}(\omega)|^2$ and $\mathcal{N}_2 \equiv N'_{\text{ph}2}(\omega) / N_{\text{ph}1}(\omega) = |T_{21}(\omega)|^2$ [Eq. (69)], are shown as functions of frequency and plate thickness for a single-slab plate in free space [$\epsilon_1(\omega) = \epsilon_3(\omega) = 1$]. The relative photon-number density of the radiation absorbed by the plate, $\mathcal{N}_a = \{N_{\text{ph}1}(\omega) - [N'_{\text{ph}1}(\omega) + N'_{\text{ph}2}(\omega)]\} / N_{\text{ph}1}(\omega) = \alpha_1(\omega) = \alpha_2(\omega)$ is shown in Fig. 5. The results in Figs. 3–5 are given for a simple model permittivity $\epsilon(\omega) \equiv \epsilon_2(\omega)$ based on a single medium resonance,

$$\epsilon(\omega) = 1 + \frac{\omega_1^2}{\omega_0^2 - \omega^2 - i\Gamma\omega}, \quad (71)$$

which enables one to clearly distinguish the (resonance) region of frequency for which the imaginary part of the refractive index may substantially exceed the real part from other (off-resonance) regions for which the imaginary part becomes small.

For frequencies that are small compared with the medium resonance frequency ($\omega \ll \omega_0$) the approximately real refrac-

tive index [$n(\omega) = \beta(\omega) + i\gamma(\omega) \approx \beta(\omega) \gg 1$] gives rise to a variation with the plate thickness of the transmitted and reflected numbers of photons which show the oscillating behavior typical for a Fabry-Pérot device. In this frequency region the losses inside the plate may be disregarded. Increasing the frequency, both the real and imaginary parts of the refractive index, $\beta(\omega)$ and $\gamma(\omega)$, respectively, are increased. Increasing $\gamma(\omega)$ implies increasing probability for photon absorption in the plate. Since the number of absorbed photons increases with the thickness of the plate, the number of transmitted photons decreases with increasing plate thickness. Further, owing to the increasing absolute value of the refractive index the number of photons that are reflected is increased at the expense of the number of photons that enter the plate. The two effects mentioned become more and more pronounced as ω approaches ω_0 . In particular, in the vicinity of the medium resonance the number of reflected photons is substantially enhanced. The photons that enter the plate are absorbed over a short distance, so that the number of transmitted photons rapidly tends to zero when the thickness of the plate is increased. In this ‘‘surface regime’’ the plate behaves like a lossy mirror, the enhanced reflectivity being caused by the large absolute value of the refractive index, which results, in general, from both the real and the imaginary parts. Further increase of frequency that is associated with a decrease of the real and imaginary parts of the refractive index (region of anomalous dispersion) reduces the effects of strong reflection and absorption and the plate again becomes fractionally transparent. Needless to say, for sufficiently high frequencies when the refractive index approaches unity the plate becomes fully transparent.

It should be noted that when the input field is in the vacuum state and the dielectric plate is in thermal equilibrium, we recognize the quantum theory of thermal radiation:

$$N'_{\text{ph}i}(\omega) = \frac{\mathcal{L}}{2\pi c} \alpha_i(\omega) n_{\text{th}}(\omega) \quad (i=1,2), \quad (72)$$

where

$$\alpha_i(\omega) = \sum_{k=1}^2 |A_{ik}(\omega)|^2 \quad (73)$$

is the (i th-side) absorption coefficient of the plate, and

$$n_{\text{th}}(\omega) = \frac{1}{\exp(\hbar\omega/k_B T) - 1} \quad (74)$$

(T , temperature; k_B , Boltzmann constant; \mathcal{L} , length of the quantization volume of the radiation). The plate behaves like a thermal radiator which tends to a blackbody as the absorption becomes perfect [$\alpha_i(\omega) \rightarrow 1$]. Note that for $\mathcal{L} \rightarrow \infty$ the photon numbers per unit frequency and unit length, $N'_{\text{ph}i}(\omega)/\mathcal{L}$, remain finite.

C. Photon tunneling through absorbing barriers

Let us finally outline the problem of photon tunneling through absorbing dielectric barriers. The question of how much time is spent by a single photon in a barrier region acting as a photonic band gap has been of increasing interest and experiments have been made to observe superluminal

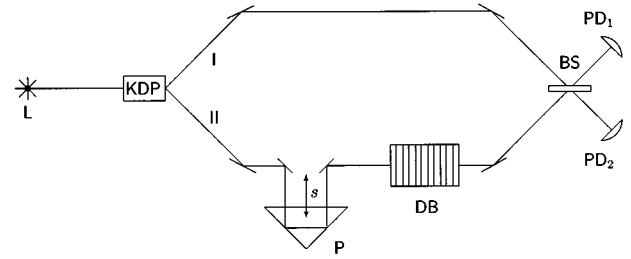


FIG. 6. Scheme of the two-photon interference experiment [24,25] for the determination of photon traversal times through multilayer dielectric barriers (L , laser; P , prism; DB , dielectric barrier; BS , beam splitter; PD_1 , PD_2 , photodetectors).

behavior of photons at such barriers [24–26], without contradiction to Einstein’s causality [27]. Although a number of theoretical predictions have been verified experimentally, there have been open questions, such as the effect of losses in the barriers.

In the experiments (Fig. 6, for details see Ref. [24]) a potassium dihydrogen phosphate (KDP) crystal is pumped by a cw UV laser, producing pairs of down-conversion photons, directed by mirrors to impinge on the surface of a 50%:50% beam splitter, the output coincidences being measured. One photon of each pair travels through air (interferometer arm I in Fig. 6), while the conjugate photon passes a multilayer dielectric barrier (interferometer arm II in Fig. 6). The coincidences attain a minimum when the two-photon wave packets overlap perfectly at the beam splitter. This can be achieved by translating an appropriately chosen prism in one arm of the interferometer in order to compensate for the delay owing to the barrier.

From photodetection theory it is well known (see, e.g., Ref. [4]) that the joint probability of recording an event in the (small) time interval t_1 , $t_1 + \Delta t_1$ and an event in the (small) time interval t_2 , $t_2 + \Delta t_2$ by the two detectors in the output channels of the interferometer is proportional to the normally ordered intensity correlation function,

$$p(t_1, t_2) = \xi^2 \Delta t_1 \Delta t_2 \langle \hat{E}'_1{}^{(-)}(x_1, t_1) \hat{E}'_2{}^{(-)}(x_2, t_2) \times \hat{E}'_2{}^{(+)}(x_2, t_2) \hat{E}'_1{}^{(+)}(x_1, t_1) \rangle \quad (75)$$

(ξ , detection efficiency). Applying the results outlined in Sec. IV A, the intensity correlation function in Eq. (75) can be related to correlation functions of the fields in the input channels of the interferometer. Whereas the action of the beam splitter simply reduces to a unitary transformation that can be assumed to be independent of frequency, the inclusion of the multilayer barrier in one arm of the interferometer requires specific knowledge of the input-output relations. To calculate the input-field correlation function, we assume that the quantum state of the correlated photon pair can be modeled by

$$|\Psi\rangle = \int_0^\infty d\Omega \left[\alpha(\Omega) \int_0^\Omega d\omega f(\omega) f(\Omega - \omega) \times \hat{a}_1^\dagger(\omega) \hat{a}_2^\dagger(\Omega - \omega) |0\rangle \right], \quad (76)$$

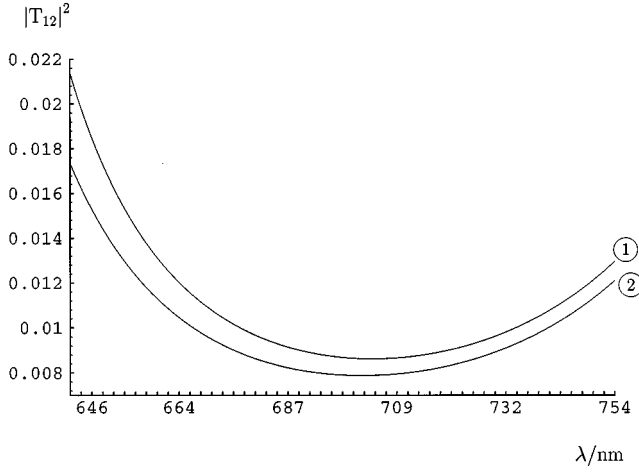


FIG. 7. The absolute value of the transmittance $|T_{12}|^2$ as a function of the wavelength λ is shown for an $H(LH)^5$ structured plate of $\lambda/4$ layers of the type described in Ref. [24]; curve (1): lossless barrier ($n_{\text{TiO}_2} = 2.22$, $n_{\text{SiO}_2} = 1.41$), curve (2): absorbing barrier ($n_{\text{TiO}_2} = 2.22$, $n_{\text{SiO}_2} = 1.41 + 0.0372i$ [29]).

where the indices I and II are used to distinguish between the two photons. The spectral interval of laser photons is given by the function $\alpha(\Omega)$, and $f(\omega)$ centered at $\Omega/2$ is the bandwidth function of the down-conversion photons. The functions $\alpha(\Omega)$ and $f(\omega)$ are normalized to unity, so that $\langle \Psi | \Psi \rangle = 1$. After some lengthy but straightforward calculation we derive the following expression for the overall coincidences R :

$$\begin{aligned}
 R &= \int dt_1 \int dt_2 p(t_1, t_2) \\
 &= 2\pi^2 \mathcal{N}^4 \int_0^\infty d\Omega \left\{ \alpha^2(\Omega) \int_{-\Omega/2}^{\Omega/2} d\omega \left(\frac{1}{4} \Omega^2 - \omega^2 \right) \right. \\
 &\quad \times f^4(\Omega/2 - \omega) T_{12}^*(\Omega/2 + \omega) \\
 &\quad \left. \times [T_{12}(\Omega/2 + \omega) - T_{12}(\Omega/2 - \omega) e^{-2i\omega\Delta\tau}] \right\} + R_{\text{th}}.
 \end{aligned} \tag{77}$$

Here, $\Delta\tau = 2s/c$, where s is the translation length of the prism, and $\mathcal{N} = \sqrt{\xi\hbar/(4\pi c\epsilon_0\mathcal{A})}$. Since the thermal contribution R_{th} is independent of s , it has not been written down explicitly.

Using the algorithm in Appendix B 2, we have performed numerical calculations for an $H(LH)^5$ structured plate (H , titanium dioxide; L , fused silica) of $\lambda/4$ layers of the type described in Ref. [24]. Restricting attention to narrow bandwidth laser light, the effect of absorption on the transmittance of the barrier and the coincidences measured is shown in Figs. 7 and 8, respectively. From these figures we see that the change in the barrier transmittance owing to an imaginary part of the refractive index of silica of about 2.6% of the real part (the data have been taken from Ref. [29]) can give rise to a shift of the position of the minimum of the coincidences of about 19%. The result indicates that the effect of losses should be considered very carefully in order to gain

deeper insight into the tunneling process. In the calculations the dependence on frequency of the refractive indices of silica and titanium dioxide has been disregarded and the refractive index of titanium dioxide has been assumed to be real, because of the lack of reliable data. In particular, the combination of the effects of dispersion and absorption is expected to affect both the delay and the curvature of the coincidences in the vicinity of the minimum, even when the changes in the refractive indices are small.

V. SUMMARY AND CONCLUSIONS

Applying the method of Green-function expansion to the quantization of radiation propagating through a multilayer dispersive and absorptive dielectric plate, we have studied the problem of calculating the proper input-output relations for the radiation-field operators and presented results for the case when the radiation propagates perpendicularly to the plate. The plate is described in terms of a multistep (spatially varying) complex permittivity in the frequency domain, which is introduced phenomenologically and only required to satisfy the Kramers-Kronig relations. The advantage of the method is that it enables one to obtain input-output relations that not only apply to regions of frequency far from the medium resonances, but are valid, within the framework of the phenomenological linear electrodynamics, in the whole frequency domain.

In consequence of the inclusion of the losses in the theory the output-radiation-field operators are found to be related to the input-radiation-field operators and operator noise sources in the plate associated with the losses, in agreement with the dissipation-fluctuation theorem. Disregarding all the losses, the characteristic absorption matrix that relates the output-radiation operators to the operator noise sources vanishes and the characteristic transformation matrix that relates the output-radiation operators to the input operators reduces to a unitary matrix. The unitary transformation ensures that the bosonic commutation relations are preserved.

When the multilayer dielectric plate is embedded in an absorbing medium the input- and output-radiation fields can be described in terms of amplitude operators whose space dependence (owing to damping) is governed by quantum Langevin equations. Only in the limiting case when the surrounding medium can be regarded as being lossless (particularly, when the plate is embedded in free space) do the amplitude operators reduce to the well-known bosonic photon operators. In this case, the characteristic transformation and absorption matrices of the plate can be shown to be related to each other through conditions that ensure preservation of the bosonic commutation relations. These conditions can be regarded as the natural generalization of the familiar unitarity conditions for lossless plates.

The input-output relations can be used advantageously in order to obtain the quantum statistics of the output radiation from that of the input radiation and the noise sources associated with the absorbing matter. In this context, we have considered normally ordered radiation-field correlation functions, with special emphasis on the spectral photon-number densities. Application of the formalism to multilayer dielectric barriers used in recent experiments on superluminal photon tunneling reveals that losses can lead to observable modifications in the delay times.

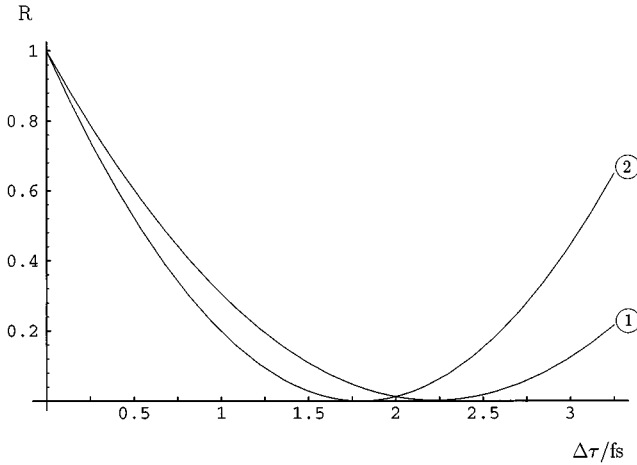


FIG. 8. The dependence on the time $\Delta\tau=2s/c$ of the coincidences R (in arbitrary units) is shown for photon tunneling through a multilayer dielectric barrier according to the scheme in Fig. 6, the transmittance of the barrier being shown in Fig. 7; curve (1): lossless barrier (minimum at 2.2 fs), curve (2): absorbing barrier (minimum at 1.8 fs).

Finally, let us briefly comment on the underlying formalism of quantization of the phenomenological Maxwell theory for radiation in dispersive and absorptive linear media. It should be mentioned that the formalism used resembles the concepts of generalized free-field theories [31]. This type of quantum field theory has recently been applied successfully to thermo field dynamics for quantum fields [32]. The similarities between the two descriptions may provide further insight into the basic physical structure of the theory, such as

the limit of vanishing absorption. In thermo field dynamics this limit corresponds to the zero-temperature limit that has been shown to be essentially nonanalytical. Similar features are also found in an indeterminacy of the dispersion relations. Absorption prevents the “spatially damped photons” from exhibiting a well-determined relation between energy (frequency) and momentum (wave vector). Similarly, at finite temperature particle states achieve a continuous spectrum not only for the particle momentum but at the same time for the mass parameter (for any fixed value of the particle momentum).

ACKNOWLEDGMENTS

We would like to thank L. Knöll for useful discussions. One of us (T.G.) is grateful to P.D. Drummond for helpful comments on the basic concepts of quantization and to P.A. Henning for the interesting discussion on thermo fields. This work was supported by the Deutsche Forschungsgemeinschaft.

APPENDIX A: SINGLE-SLAB GREEN FUNCTION

Let us consider a dielectric slab of thickness l embedded in dielectric matter that may be different on the two sides (see Fig. 1). The Green function $G(x, x', \omega)$ can be obtained from Eqs. (25), (26), and (28), with $N=3$. The coefficients $C_j^{(1)}(x', \omega)$ and $C_j^{(2)}(x', \omega)$ in Eq. (28), $j=1,2,3$, must be determined from the conditions that the Green function is continuously differentiable at the surfaces of discontinuity (that is to say, at $x = \pm l/2$) and vanishes at infinity. Note that the latter requires the coefficients $C_1^{(1)}(x', \omega)$ and $C_3^{(2)}(x', \omega)$ to be zero. Straightforward but rather lengthy calculation yields $[n_j \equiv n_j(\omega)]$

$$\begin{aligned}
G(x, x', \omega) = & \left[2in_1 \frac{\omega}{c} \right]^{-1} \Theta(-x' - \frac{1}{2}l) \{ \Theta(-x - \frac{1}{2}l) [e^{in_1\omega|x-x'|/c} + e^{in_1\omega|(-l)/2-x'|/c} \\
& \times (r_{12} + t_{12} \vartheta e^{in_2\omega l/c} r_{23} e^{in_2\omega l/c} t_{21}) e^{in_1\omega|(-l)/2-x|/c}] + [\Theta(x + \frac{1}{2}l) - \Theta(x - \frac{1}{2}l)] t_{12} \vartheta e^{in_1\omega|(-l)/2-x'|/c} \\
& \times (e^{in_2\omega|x-(-l)/2|/c} + r_{23} e^{in_2\omega(l+|l/2-x|/c)}) + \Theta(x - \frac{1}{2}l) e^{in_1\omega|(-l)/2-x'|/c} t_{12} e^{in_2\omega l/c} \vartheta t_{23} e^{in_3\omega|x-l/2|/c} \} \\
& + \left[2in_2 \frac{\omega}{c} \right]^{-1} \\
& \times [\Theta(x' + \frac{1}{2}l) - \Theta(x' - \frac{1}{2}l)] \{ \Theta(-x - \frac{1}{2}l) \vartheta (e^{in_2\omega|x'-(-l)/2|/c} + e^{in_2\omega|l/2-x'|/c} r_{23} e^{in_2\omega l/c}) t_{21} e^{in_1\omega|(-l)/2-x|/c} \\
& + [\Theta(x + \frac{1}{2}l) - \Theta(x - \frac{1}{2}l)] [e^{in_2\omega|x-x'|/c} + \vartheta (e^{in_2\omega|x'-(-l)/2|/c} r_{21} e^{in_2\omega l/c} + e^{in_2\omega|l/2-x'|/c} r_{23} e^{in_2\omega|l/2-x|/c} \\
& + \vartheta (e^{in_2\omega|x'-(-l)/2|/c} + e^{in_2\omega|l/2-x'|/c} r_{23} e^{in_2\omega l/c}) r_{21} e^{in_2\omega|x-(-l)/2|/c}] \\
& + \Theta(x - \frac{1}{2}l) \vartheta (e^{in_2\omega|x'-(-l)/2|/c} r_{21} e^{in_2\omega l/c} + e^{in_2\omega|l/2-x'|/c}) t_{23} e^{in_3\omega|x-l/2|/c} \} + \left[2in_3 \frac{\omega}{c} \right]^{-1} \Theta(x' - \frac{1}{2}l) \\
& \times \{ \Theta(-x - \frac{1}{2}l) e^{in_3\omega|x'-l/2|/c} t_{32} \vartheta e^{in_2\omega l/c} t_{21} e^{in_1\omega|(-l)/2-x|/c} + [\Theta(x + \frac{1}{2}l) - \Theta(x - \frac{1}{2}l)] e^{in_3\omega|x'-l/2|/c} \\
& \times t_{32} \vartheta (e^{in_2\omega|l/2-x|/c} + e^{in_2\omega l/c} r_{21} e^{in_2\omega|x-(-l)/2|/c}) + \Theta(x - \frac{1}{2}l) [e^{in_3\omega|x-x'|/c} + e^{in_3\omega|x'-l/2|/c} \\
& \times (r_{32} + t_{32} \vartheta e^{in_2\omega l/c} r_{21} e^{in_2\omega l/c} t_{23}) e^{in_3\omega|x-l/2|/c} \} \}. \tag{A1}
\end{aligned}$$

Here, the interface reflection and transmission coefficients $r_{ij} \equiv r_{ij}(\omega)$ and $t_{ij} \equiv t_{ij}(\omega)$, respectively, are defined by

$$r_{ij}(\omega) = -r_{ji}(\omega) = \frac{n_i(\omega) - n_j(\omega)}{n_i(\omega) + n_j(\omega)}, \quad (\text{A2})$$

$$t_{ij}(\omega) = \frac{2n_i(\omega)}{n_i(\omega) + n_j(\omega)}, \quad (\text{A3})$$

and the factor $\vartheta \equiv \vartheta(\omega)$, which arises from multiple reflections inside the slab, reads as

$$\begin{aligned} \vartheta(\omega) &= \sum_{j=0}^{\infty} [e^{in_2(\omega)\omega l/c} r_{21}(\omega) e^{in_2(\omega)\omega l/c} r_{23}(\omega)]^j \\ &= [1 - e^{in_2(\omega)\omega l/c} r_{21}(\omega) e^{in_2(\omega)\omega l/c} r_{23}(\omega)]^{-1}. \end{aligned} \quad (\text{A4})$$

Note that the above given form of the Green function permits of a direct physical interpretation. The terms in Eq. (A1) simply correspond to the potential propagations of radiation from a source point x' to a point of observation, x .

$[n_j(\omega) = \beta_j(\omega) + i\gamma_j(\omega)]$, and the amplitude operators of the outgoing fields to the left and right, respectively, $\hat{a}_{1-}(x, \omega)$ and $\hat{a}_{3+}(x, \omega)$, are given by

$$\begin{aligned} \hat{a}_{1-}(x, \omega) &= \frac{1}{i} \sqrt{2\gamma_1(\omega)} \frac{\omega}{c} e^{\gamma_1(\omega)\omega x/c} \int_x^{-l/2} dx' e^{in_1(\omega)\omega x'/c} \hat{f}(x', \omega) + e^{\gamma_1(\omega)\omega(x-l/2)/c} e^{-in_1(\omega)\omega l/c} \\ &\quad \times [r_{12}(\omega) + t_{12}(\omega)r_{23}(\omega)t_{21}(\omega) e^{2in_2(\omega)\omega l/c} \vartheta(\omega)] \hat{a}_{1+}(-\frac{1}{2}l, \omega) + \sqrt{2\gamma_1(\omega)} e^{\gamma_1(\omega)\omega x/c} \frac{n_1(\omega)}{n_2(\omega)} \sqrt{\frac{\beta_2(\omega)\gamma_2(\omega)}{\beta_1(\omega)\gamma_1(\omega)}} \\ &\quad \times \vartheta(\omega)t_{21}(\omega) e^{-in_1(\omega)\omega l/(2c)} [\hat{g}'_-(\omega) + r_{23}(\omega) e^{in_2(\omega)\omega l/c} \hat{g}'_+(\omega)] + e^{[\gamma_1(\omega)x - \gamma_3(\omega)l/2]\omega/c} \frac{n_1(\omega)}{n_3(\omega)} \sqrt{\frac{\beta_3(\omega)}{\beta_1(\omega)}} \\ &\quad \times e^{-i[n_1(\omega) - 2n_2(\omega) + n_3(\omega)]\omega l/(2c)} t_{32}(\omega)t_{21}(\omega) \vartheta(\omega) \hat{a}_{3-}(\frac{1}{2}l, \omega), \end{aligned} \quad (\text{B3})$$

$$\begin{aligned} \hat{a}_{3+}(x, \omega) &= \frac{1}{i} \sqrt{2\gamma_3(\omega)} \frac{\omega}{c} e^{-\gamma_3(\omega)\omega x/c} \int_{l/2}^x dx' e^{-in_3(\omega)\omega x'/c} \hat{f}(x', \omega) + e^{-\gamma_3(\omega)\omega(x+l/2)/c} e^{-in_3(\omega)\omega l/c} \\ &\quad \times [r_{32}(\omega) + t_{32}(\omega)r_{21}(\omega)t_{23}(\omega) e^{2in_2(\omega)\omega l/c} \vartheta(\omega)] \hat{a}_{3-}(\frac{1}{2}l, \omega) + \sqrt{2\gamma_3(\omega)} e^{-\gamma_3(\omega)\omega x/c} \frac{n_3(\omega)}{n_2(\omega)} \sqrt{\frac{\beta_2(\omega)\gamma_2(\omega)}{\beta_3(\omega)\gamma_3(\omega)}} \\ &\quad \times \vartheta(\omega)t_{23}(\omega) e^{-in_3(\omega)\omega l/(2c)} [\hat{g}'_+(\omega) + r_{21}(\omega) e^{in_2(\omega)\omega l/c} \hat{g}'_-(\omega)] + e^{-[\gamma_1(\omega)l/2 + \gamma_3(\omega)x]\omega/c} \frac{n_3(\omega)}{n_1(\omega)} \sqrt{\frac{\beta_1(\omega)}{\beta_3(\omega)}} \\ &\quad \times e^{-i[n_1(\omega) - 2n_2(\omega) + n_3(\omega)]\omega l/(2c)} t_{12}(\omega)t_{23}(\omega) \vartheta(\omega) \hat{a}_{1+}(-\frac{1}{2}l, \omega), \end{aligned} \quad (\text{B4})$$

where the operators $\hat{g}'_{\pm}(\omega)$ are defined in Eq. (36).

Inverting the relations (35), we may express the operators $\hat{g}'_{\pm}(\omega)$ in terms of the operators $\hat{g}_{\pm}^{(1)}(\omega)$ and rewrite Eqs. (B3) (for $x = -l/2$) and (B4) (for $x = l/2$) in the compact form

$$\begin{pmatrix} \hat{a}_{1-}(-\frac{1}{2}l, \omega) \\ \hat{a}_{3+}(\frac{1}{2}l, \omega) \end{pmatrix} = \tilde{\mathbf{T}}^{(1)} \begin{pmatrix} \hat{a}_{1+}(-\frac{1}{2}l, \omega) \\ \hat{a}_{3-}(\frac{1}{2}l, \omega) \end{pmatrix} + \tilde{\mathbf{A}}^{(1)} \begin{pmatrix} \hat{g}_{+}^{(1)}(\omega) \\ \hat{g}_{-}^{(1)}(\omega) \end{pmatrix}. \quad (\text{B5})$$

The elements of the characteristic transformation matrix $\tilde{\mathbf{T}}^{(1)}$, $T_{ik}^{(1)}(\omega)$, are seen to be

APPENDIX B: PHOTONIC OPERATORS, NOISE OPERATORS, INPUT-OUTPUT RELATIONS

1. Single-slab dielectric plate

Substituting in Eq. (9) for $G(x, x', \omega)$ the expression (A1) and rewriting the result (within the space intervals $-\infty \leq x \leq -l/2$ and $l/2 \leq x \leq \infty$) in the form (29), we easily see that the amplitude operators of the incoming fields from the left and right, respectively, $\hat{a}_{1+}(x, \omega)$ and $\hat{a}_{3-}(x, \omega)$, read as

$$\begin{aligned} \hat{a}_{1+}(x, \omega) &= \frac{1}{i} \sqrt{2\gamma_1(\omega)} \frac{\omega}{c} e^{-\gamma_1(\omega)\omega x/c} \\ &\quad \times \int_{-\infty}^x dx' e^{-in_1(\omega)\omega x'/c} \hat{f}(x', \omega), \end{aligned} \quad (\text{B1})$$

$$\begin{aligned} \hat{a}_{3-}(x, \omega) &= \frac{1}{i} \sqrt{2\gamma_3(\omega)} \frac{\omega}{c} e^{\gamma_3(\omega)\omega x/c} \\ &\quad \times \int_x^{\infty} dx' e^{in_3(\omega)\omega x'/c} \hat{f}(x', \omega) \end{aligned} \quad (\text{B2})$$

$$T_{11}^{(1)}(\omega) = e^{-i\beta_1(\omega)\omega l/c} [r_{12}(\omega) + t_{12}(\omega)e^{2in_2(\omega)\omega l/c} r_{23}(\omega) \vartheta(\omega) t_{21}(\omega)], \tag{B6}$$

$$T_{12}^{(1)}(\omega) = \frac{n_1(\omega)}{n_3(\omega)} \sqrt{\frac{\beta_3(\omega)}{\beta_1(\omega)}} e^{-i[\beta_1(\omega) + \beta_3(\omega)]\omega l/(2c)} t_{32}(\omega) e^{in_2(\omega)\omega l/c} \vartheta(\omega) t_{21}(\omega), \tag{B7}$$

$$T_{21}^{(1)}(\omega) = \frac{n_3(\omega)}{n_1(\omega)} \sqrt{\frac{\beta_1(\omega)}{\beta_3(\omega)}} e^{-i[\beta_1(\omega) + \beta_3(\omega)]\omega l/(2c)} t_{12}(\omega) e^{in_2(\omega)\omega l/c} \vartheta(\omega) t_{23}(\omega), \tag{B8}$$

$$T_{22}^{(1)}(\omega) = e^{-i\beta_3(\omega)\omega l/c} [r_{32}(\omega) + t_{32}(\omega)e^{2in_2(\omega)\omega l/c} r_{21}(\omega) \vartheta(\omega) t_{23}(\omega)], \tag{B9}$$

and the elements of the characteristic absorption matrix $\tilde{\mathbf{A}}^{(1)}$, $A_{ik}^{(1)}(\omega)$, read as

$$A_{11}^{(1)}(\omega) = \sqrt{\gamma_2(\omega) \frac{\beta_2(\omega)}{\beta_1(\omega)}} e^{-i\beta_1(\omega)\omega l/(2c)} t_{12}(\omega) \vartheta(\omega) \times \sqrt{c_+} [1 + e^{in_2(\omega)\omega l/c} r_{23}(\omega)], \tag{B10}$$

$$A_{12}^{(1)}(\omega) = \sqrt{\gamma_2(\omega) \frac{\beta_2(\omega)}{\beta_1(\omega)}} e^{-i\beta_1(\omega)\omega l/(2c)} t_{12}(\omega) \vartheta(\omega) \times \sqrt{c_-} [1 - e^{in_2(\omega)\omega l/c} r_{23}(\omega)], \tag{B11}$$

$$A_{21}^{(1)}(\omega) = \sqrt{\gamma_2(\omega) \frac{\beta_2(\omega)}{\beta_3(\omega)}} e^{-i\beta_3(\omega)\omega l/(2c)} t_{32}(\omega) \vartheta(\omega) \times \sqrt{c_+} [e^{in_2(\omega)\omega l/c} r_{21}(\omega) + 1], \tag{B12}$$

$$A_{22}^{(1)}(\omega) = \sqrt{\gamma_2(\omega) \frac{\beta_2(\omega)}{\beta_3(\omega)}} e^{-i\beta_3(\omega)\omega l/(2c)} t_{32}(\omega) \vartheta(\omega) \times \sqrt{c_-} [e^{in_2(\omega)\omega l/c} r_{21}(\omega) - 1], \tag{B13}$$

where c_{\pm} is defined in Eq. (37).

Note that when the plate is surrounded by vacuum,

$$n_1(\omega) = n_3(\omega) \equiv 1, \tag{B14}$$

so that

$$\beta_1(\omega) = \beta_3(\omega) \equiv 1, \quad \gamma_1(\omega) = \gamma_3(\omega) \equiv 0, \tag{B15}$$

the following relations are valid [cf. Eqs. (A2)–(A4)]:

$$r_{12}(\omega) = r_{32}(\omega) = \frac{1 - n_2(\omega)}{1 + n_2(\omega)} = -r_{21}(\omega) = -r_{23}(\omega), \tag{B16}$$

$$t_{12}(\omega) = t_{32}(\omega) = \frac{2}{1 + n_2(\omega)}, \tag{B17}$$

$$t_{21}(\omega) = t_{23}(\omega) = \frac{2n_2(\omega)}{1 + n_2(\omega)}, \tag{B18}$$

$$\vartheta(\omega) = \sum_{j=0}^{\infty} [e^{in_2(\omega)\omega l/c} r_{21}(\omega) e^{in_2(\omega)\omega l/c} r_{23}(\omega)]^j = [1 - r_{21}^2(\omega) e^{2in_2(\omega)\omega l/c}]^{-1}. \tag{B19}$$

Using Eqs. (35) and (36) and recalling the commutation relations (6) and (7), from Eqs. (B1) and (B2) we derive that

$$[\hat{a}_{1+}(x, \omega), \hat{a}_{1+}^\dagger(x', \omega')] = e^{-\gamma_1(\omega)\omega |x-x'|/c} \delta(\omega - \omega'), \tag{B20}$$

$$[\hat{a}_{3-}(x, \omega), \hat{a}_{3-}^\dagger(x', \omega')] = e^{-\gamma_3(\omega)\omega |x-x'|/c} \delta(\omega - \omega'), \tag{B21}$$

$$[\hat{a}_{1+}(x, \omega), \hat{a}_{3-}^\dagger(x', \omega')] = 0, \tag{B22}$$

$$[\hat{a}_{1+}(x, \omega), (\hat{g}_{\pm}^{(1)}(\omega'))^\dagger] = 0 = [\hat{a}_{3-}(x, \omega), (\hat{g}_{\pm}^{(1)}(\omega'))^\dagger]. \tag{B23}$$

The commutation relations for the output amplitude operators $\hat{a}_{1-}(x, \omega)$, $\hat{a}_{3+}(x, \omega)$ and $\hat{a}_{1-}^\dagger(x, \omega)$, $\hat{a}_{3+}^\dagger(x, \omega)$ can be derived in a similar way or, more easily, using Eqs. (30) and (31) and applying the input-output relations (B5) (together with the corresponding commutation relations). Straightforward calculation yields

$$\begin{aligned}
[\hat{a}_{1-}(x, \omega), \hat{a}_{1-}^\dagger(x', \omega')] &= \delta(\omega - \omega') \left\{ e^{-\gamma_1(\omega)\omega|x-x'|/c} + e^{-\gamma_1(\omega)\omega[|x-(-l/2)|/c + |x'-(-l/2)|/c]} \right. \\
&\times \left[|T_{11}^{(1)}(\omega)|^2 + |T_{12}^{(1)}(\omega)|^2 + |A_{11}^{(1)}(\omega)|^2 + |A_{12}^{(1)}(\omega)|^2 - 1 + i \frac{\gamma_1(\omega)}{\beta_1(\omega)} \right. \\
&\times \left. \left. \left\{ T_{11}^{(1)}(\omega)(e^{i\beta_1(\omega)\omega l/c} - e^{-2i\beta_1(\omega)\omega x'/c}) - [T_{11}^{(1)}(\omega)]^*(e^{-i\beta_1(\omega)\omega l/c} - e^{2i\beta_1(\omega)\omega x/c}) \right\} \right] \right\}, \quad (\text{B24})
\end{aligned}$$

$$\begin{aligned}
[\hat{a}_{3+}(x, \omega), \hat{a}_{3+}^\dagger(x', \omega')] &= \delta(\omega - \omega') \left\{ e^{-\gamma_3(\omega)\omega|x-x'|/c} + e^{-\gamma_3(\omega)\omega[|x-l/2|/c + |x'-l/2|/c]} \right. \\
&\times \left[|T_{21}^{(1)}(\omega)|^2 + |T_{22}^{(1)}(\omega)|^2 + |A_{21}^{(1)}(\omega)|^2 + |A_{22}^{(1)}(\omega)|^2 - 1 + i \frac{\gamma_3(\omega)}{\beta_3(\omega)} \right. \\
&\times \left. \left. \left\{ T_{22}^{(1)}(\omega)(e^{i\beta_3(\omega)\omega l/c} - e^{2i\beta_3(\omega)\omega x'/c}) - [T_{22}^{(1)}(\omega)]^*(e^{-i\beta_3(\omega)\omega l/c} - e^{-2i\beta_3(\omega)\omega x/c}) \right\} \right] \right\}, \quad (\text{B25})
\end{aligned}$$

$$\begin{aligned}
[\hat{a}_{3+}(x, \omega), \hat{a}_{1-}^\dagger(x', \omega')] &= \delta(\omega - \omega') \left\{ e^{-\gamma_1(\omega)\omega|x'-(-l/2)|/c - \gamma_3(\omega)\omega|x-l/2|/c} \left[[T_{11}^{(1)}(\omega)]^* T_{21}^{(1)}(\omega) \right. \right. \\
&+ [T_{12}^{(1)}(\omega)]^* T_{22}^{(1)}(\omega) + [A_{11}^{(1)}(\omega)]^* A_{21}^{(1)}(\omega) + [A_{12}^{(1)}(\omega)]^* A_{22}^{(1)}(\omega) \\
&+ iT_{21}^{(1)}(\omega) \frac{\gamma_1(\omega)}{\beta_1(\omega)} (e^{i\beta_1(\omega)\omega l/c} - e^{-2i\beta_1(\omega)\omega x'/c}) \\
&\left. \left. + i[T_{12}^{(1)}(\omega)]^* \frac{\gamma_3(\omega)}{\beta_3(\omega)} (e^{-2i\beta_3(\omega)\omega x/c} - e^{-i\beta_3(\omega)\omega l/c}) \right] \right\}. \quad (\text{B26})
\end{aligned}$$

Needless to say, $\hat{a}_{1-}(x, \omega)$ and $\hat{a}_{3+}(x, \omega)$ are commuting quantities. Using Eqs. (B6)–(B13) and assuming that the plate is embedded in nonabsorbing media [$\gamma_1(\omega) = \gamma_3(\omega) = 0$], the following relations are easily proved correct:

$$\begin{aligned}
&|T_{11}^{(1)}(\omega)|^2 + |T_{12}^{(1)}(\omega)|^2 + |A_{11}^{(1)}(\omega)|^2 + |A_{12}^{(1)}(\omega)|^2 \\
&= |T_{21}^{(1)}(\omega)|^2 + |T_{22}^{(1)}(\omega)|^2 + |A_{21}^{(1)}(\omega)|^2 + |A_{22}^{(1)}(\omega)|^2 = 1, \quad (\text{B27})
\end{aligned}$$

$$\begin{aligned}
&T_{11}^{(1)}(\omega)[T_{21}^{(1)}(\omega)]^* + T_{12}^{(1)}(\omega)[T_{22}^{(1)}(\omega)]^* \\
&+ A_{11}^{(1)}(\omega)[A_{21}^{(1)}(\omega)]^* + A_{12}^{(1)}(\omega)[A_{22}^{(1)}(\omega)]^* = 0. \quad (\text{B28})
\end{aligned}$$

In this case, both the input-field commutation relations (B20)–(B22) and the output-field commutation relations

(B24)–(B26) obviously reduce to the familiar bosonic commutation relations for photon destruction and creation operators.

2. Multislabs dielectric plates

Starting from the results derived in Appendix B 1 for a single-slab dielectric plate ($N=3$), the results for an arbitrary dielectric plate ($N \geq 3$, cf. Fig. 2) can be obtained step by step, without explicitly calculating the multislabs Green function. For this purpose we show that when Eqs. (44)–(50) are valid for $N-1$, then they are also valid for N . Using Eq. (44), with $N-1$ in place of N , and expressing the operators $\hat{a}_{N-1 \pm}(x_{N-2}, \omega)$ in terms of the operators $\hat{a}_{1 \pm}(x_1, \omega)$, we find that

$$\begin{aligned}
\begin{pmatrix} \hat{a}_{N-1+}(x_{N-2}, \omega) \\ \hat{a}_{N-1-}(x_{N-2}, \omega) \end{pmatrix} &= \tilde{\mathbf{P}} \begin{pmatrix} \hat{a}_{1-}(x_1, \omega) \\ \hat{a}_{1+}(x_1, \omega) \end{pmatrix} \\
&+ \tilde{\mathbf{Q}} \begin{pmatrix} \hat{g}_+^{(N-3)}(\omega) \\ \hat{g}_-^{(N-3)}(\omega) \end{pmatrix}, \quad (\text{B29})
\end{aligned}$$

where the matrices $\tilde{\mathbf{P}} \equiv \tilde{\mathbf{P}}^{(N-3)}$ and $\tilde{\mathbf{Q}} \equiv \tilde{\mathbf{Q}}^{(N-3)}$ are given by

$$\tilde{\mathbf{P}} = (T_{12}^{(N-3)})^{-2} \begin{pmatrix} T_{22}^{(N-3)} & T_{21}^{(N-3)} T_{12}^{(N-3)} - T_{22}^{(N-3)} T_{11}^{(N-3)} \\ 1 & -T_{11}^{(N-3)} \end{pmatrix}, \quad (\text{B30})$$

$$\tilde{\mathbf{Q}} = (T_{12}^{(N-3)})^{-2} \begin{pmatrix} A_{21}^{(N-3)} T_{12}^{(N-3)} - A_{11}^{(N-3)} T_{22}^{(N-3)} & A_{22}^{(N-3)} T_{12}^{(N-3)} - A_{12}^{(N-3)} T_{22}^{(N-3)} \\ -A_{11}^{(N-3)} & -A_{12}^{(N-3)} \end{pmatrix}. \quad (\text{B31})$$

The desired $(N-2)$ -slab plate can be obtained by supplement to the $(N-3)$ -slab plate of the $(N-1)$ th slab (cf. Fig. 2). Applying Eq. (30) to $\hat{a}_{N-1\pm}(x, \omega)$ ($x_{N-2} \leq x \leq x_{N-1}$) yields

$$\hat{a}_{N-1\pm}(x_{N-1}, \omega) = \hat{a}_{N-1\pm}(x_{N-2}, \omega) e^{\mp \gamma_{N-1}(\omega) \omega l_{N-1}/c} + \hat{d}'_{N-1\pm}(\omega), \quad (\text{B32})$$

where $l_{N-1} = x_{N-1} - x_{N-2}$, and

$$\hat{d}'_{N-1\pm}(\omega) = \int_{x_{N-2}}^{x_{N-1}} dy \hat{F}_{N-1\pm}(y, \omega) e^{\mp \gamma_{N-1}(\omega) \omega (x_{N-1}-y)/c}, \quad (\text{B33})$$

with $\hat{F}_{N-1\pm}(y, \omega)$ according to Eq. (31). Recalling the commutation relations (21), the operators $\hat{d}'_{N-1\pm}$ are found to satisfy the commutation relations

$$[\hat{d}'_{N-1\pm}(\omega), \hat{d}'_{N-1\pm}(\omega')] = 2\delta(\omega - \omega') e^{\mp \gamma_{N-1}(\omega) \omega l_{N-1}/c} \times \sinh\left[\gamma_{N-1}(\omega) \frac{\omega}{c} l_{N-1}\right], \quad (\text{B34})$$

$$[\hat{d}'_{N-1\pm}(\omega), \hat{d}'_{N-1\mp}(\omega')] = -2\delta(\omega - \omega') \frac{\gamma_{N-1}(\omega)}{\beta_{N-1}(\omega)} \times e^{\mp i\beta_{N-1}(\omega) \omega (x_{N-2} + x_{N-1})/c} \times \sin\left[\beta_{N-1}(\omega) \frac{\omega}{c} l_{N-1}\right]. \quad (\text{B35})$$

By means of linear combination of the operators $\hat{d}'_{N-1\pm}$, bosonic operators $\hat{d}_{N-1\pm}$ can be introduced as

$$\begin{pmatrix} \hat{d}_{N-1+}(\omega) \\ \hat{d}_{N-1-}(\omega) \end{pmatrix} = \tilde{\mathbf{D}} \begin{pmatrix} \hat{d}'_{N-1+}(\omega) \\ \hat{d}'_{N-1-}(\omega) \end{pmatrix}, \quad (\text{B36})$$

$$[\hat{d}_{N-1\pm}(\omega), \hat{d}_{N-1\pm}(\omega')] = \delta(\omega - \omega'), \quad (\text{B37})$$

$$[\hat{d}_{N-1\pm}(\omega), \hat{d}_{N-1\mp}(\omega')] = 0. \quad (\text{B38})$$

In Eq. (B36), the matrix $\tilde{\mathbf{D}}$ reads as

$$D_{11} = \left\{ 2 \left[\alpha_+ + \left(\frac{\alpha_+}{\alpha_-} \right)^{1/2} |\alpha_0| \right] \right\}^{-1/2}, \quad (\text{B39})$$

$$D_{21} = - \left\{ 2 \left[\alpha_+ - \left(\frac{\alpha_+}{\alpha_-} \right)^{1/2} |\alpha_0| \right] \right\}^{-1/2}, \quad (\text{B40})$$

$$D_{12} = \exp[i \arg(\alpha_0)] \left\{ 2 \left[\alpha_- + \left(\frac{\alpha_-}{\alpha_+} \right)^{1/2} |\alpha_0| \right] \right\}^{-1/2}, \quad (\text{B41})$$

$$D_{22} = \exp[i \arg(\alpha_0)] \left\{ 2 \left[\alpha_- - \left(\frac{\alpha_-}{\alpha_+} \right)^{1/2} |\alpha_0| \right] \right\}^{-1/2}, \quad (\text{B42})$$

where

$$\alpha_{\pm} = 2e^{\mp \gamma_{N-1}(\omega) \omega l_{N-1}/c} \sinh\left[\gamma_{N-1}(\omega) \frac{\omega}{c} l_{N-1}\right], \quad (\text{B43})$$

$$\alpha_0 = -2 \frac{\gamma_{N-1}(\omega)}{\beta_{N-1}(\omega)} e^{-i\beta_{N-1}(\omega) \omega (x_{N-2} + x_{N-1})/c} \times \sin\left[\beta_{N-1}(\omega) \frac{\omega}{c} l_{N-1}\right]. \quad (\text{B44})$$

Combining Eqs. (B32) and (B36) we may write

$$\begin{pmatrix} \hat{a}_{N-1+}(x_{N-1}, \omega) \\ \hat{a}_{N-1-}(x_{N-1}, \omega) \end{pmatrix} = \tilde{\mathbf{R}} \begin{pmatrix} \hat{a}_{N-1+}(x_{N-2}, \omega) \\ \hat{a}_{N-1-}(x_{N-2}, \omega) \end{pmatrix} + \tilde{\mathbf{D}}^{-1} \begin{pmatrix} \hat{d}_{N-1+}(\omega) \\ \hat{d}_{N-1-}(\omega) \end{pmatrix}, \quad (\text{B45})$$

where $R_{ii'} = R_{ii} \delta_{ii'}$, with

$$R_{11} = R_{22}^{-1} = \exp\left[-\gamma_{N-1}(\omega) \frac{\omega}{c} l_{N-1}\right]. \quad (\text{B46})$$

We now relate the operators $\hat{a}_{N\pm}(x_{N-1}, \omega)$ and $\hat{a}_{N-1\pm}(x_{N-1}, \omega)$ to each other, recalling that $\hat{A}(x)$ is continuously differentiable at x_{N-1} . Straightforward calculation yields

$$\begin{pmatrix} \hat{a}_{N+}(x_{N-1}, \omega) \\ \hat{a}_{N-}(x_{N-1}, \omega) \end{pmatrix} = \tilde{\mathbf{S}} \begin{pmatrix} \hat{a}_{N-1+}(x_{N-1}, \omega) \\ \hat{a}_{N-1-}(x_{N-1}, \omega) \end{pmatrix}, \quad (\text{B47})$$

where the elements of the matrix $\tilde{\mathbf{S}}$ read as

$$S_{11} = \sqrt{\frac{\beta_{N-1}(\omega) n_N(\omega) + n_{N-1}(\omega)}{\beta_N(\omega) 2n_{N-1}(\omega)}} \times e^{-i[\beta_N(\omega) - \beta_{N-1}(\omega)] \omega x_{N-1}/c}, \quad (\text{B48})$$

$$S_{12} = \sqrt{\frac{\beta_{N-1}(\omega) n_N(\omega) - n_{N-1}(\omega)}{\beta_N(\omega) 2n_{N-1}(\omega)}} \times e^{-i[\beta_N(\omega) + \beta_{N-1}(\omega)]\omega x_{N-1}/c}, \quad (\text{B49})$$

$$S_{21} = \sqrt{\frac{\beta_{N-1}(\omega) n_N(\omega) - n_{N-1}(\omega)}{\beta_N(\omega) 2n_{N-1}(\omega)}} \times e^{i[\beta_N(\omega) + \beta_{N-1}(\omega)]\omega x_{N-1}/c}, \quad (\text{B50})$$

$$S_{22} = \sqrt{\frac{\beta_{N-1}(\omega) n_N(\omega) + n_{N-1}(\omega)}{\beta_N(\omega) 2n_{N-1}(\omega)}} \times e^{i[\beta_N(\omega) - \beta_{N-1}(\omega)]\omega x_{N-1}/c}. \quad (\text{B51})$$

Combining Eqs. (B29), (B45), and (B47), we obtain

$$\begin{pmatrix} \hat{a}_{N+}(x_{N-1}, \omega) \\ \hat{a}_{N-}(x_{N-1}, \omega) \end{pmatrix} = \widetilde{\text{SRP}} \begin{pmatrix} \hat{a}_{1-}(x_1, \omega) \\ \hat{a}_{1+}(x_1, \omega) \end{pmatrix} + \widetilde{\text{SRQ}} \begin{pmatrix} \hat{g}_+^{(N-3)}(\omega) \\ \hat{g}_-^{(N-3)}(\omega) \end{pmatrix} + \widetilde{\text{SD}}^{-1} \begin{pmatrix} \hat{d}_{N-1+}(\omega) \\ \hat{d}_{N-1-}(\omega) \end{pmatrix}, \quad (\text{B52})$$

from which we deduce that

$$\begin{pmatrix} \hat{a}_{1-}(x_1, \omega) \\ \hat{a}_{N+}(x_{N-1}, \omega) \end{pmatrix} = \widetilde{\text{T}}^{(N-2)} \begin{pmatrix} \hat{a}_{1+}(x_1, \omega) \\ \hat{a}_{N-}(x_{N-1}, \omega) \end{pmatrix} + \widetilde{\text{A}}' \begin{pmatrix} \hat{g}_+^{(N-3)}(\omega) \\ \hat{g}_-^{(N-3)}(\omega) \end{pmatrix} + \widetilde{\text{A}}'' \begin{pmatrix} \hat{d}_{N-1+}(\omega) \\ \hat{d}_{N-1-}(\omega) \end{pmatrix}, \quad (\text{B53})$$

where the matrices read as

$$\widetilde{\text{T}}^{(N-2)} = (\text{SRP})_{21}^{-2} \begin{pmatrix} -(\text{SRP})_{22} & 1 \\ (\text{SRP})_{12}(\text{SRP})_{21} - (\text{SRP})_{11}(\text{SRP})_{22} & (\text{SRP})_{11} \end{pmatrix}, \quad (\text{B54})$$

$$\widetilde{\text{A}}' = (\text{SRP})_{21}^{-2} \begin{pmatrix} -(\text{SRQ})_{21} & -(\text{SRQ})_{22} \\ (\text{SRQ})_{11}(\text{SRP})_{21} - (\text{SRQ})_{21}(\text{SRP})_{11} & (\text{SRQ})_{12}(\text{SRP})_{21} - (\text{SRQ})_{22}(\text{SRP})_{11} \end{pmatrix}, \quad (\text{B55})$$

$$\widetilde{\text{A}}'' = (\text{SRP})_{21}^{-2} \begin{pmatrix} -(\text{SD}^{-1})_{21} & -(\text{SD}^{-1})_{22} \\ (\text{SD}^{-1})_{11}(\text{SRP})_{21} - (\text{SD}^{-1})_{21}(\text{SRP})_{11} & (\text{SD}^{-1})_{12}(\text{SRP})_{21} - (\text{SD}^{-1})_{22}(\text{SRP})_{11} \end{pmatrix}. \quad (\text{B56})$$

Note that $\hat{g}_\pm^{(N-3)}(\omega)$ and $\hat{d}_{N-1\pm}^\dagger(\omega)$ are commuting quantities, because they refer to different space intervals [cf. the commutation relations (6) or (21)].

Finally, we introduce bosonic operators $\hat{g}_\pm^{(N-2)}(\omega)$ as linear combinations of the operators $\hat{g}_\pm^{(N-3)}(\omega)$ and $\hat{d}_{N-1\pm}(\omega)$:

$$\begin{pmatrix} \hat{g}_+^{(N-2)}(\omega) \\ \hat{g}_-^{(N-2)}(\omega) \end{pmatrix} = \widetilde{\text{U}} \left[\widetilde{\text{A}}' \begin{pmatrix} \hat{g}_+^{(N-3)}(\omega) \\ \hat{g}_-^{(N-3)}(\omega) \end{pmatrix} + \widetilde{\text{A}}'' \begin{pmatrix} \hat{d}_{N-1+}(\omega) \\ \hat{d}_{N-1-}(\omega) \end{pmatrix} \right], \quad (\text{B57})$$

$$[\hat{g}_\pm^{(N-2)}(\omega), (\hat{g}_\pm^{(N-2)}(\omega'))^\dagger] = \delta(\omega - \omega'), \quad (\text{B58})$$

$$[\hat{g}_\pm^{(N-2)}(\omega), (\hat{g}_\mp^{(N-2)}(\omega'))^\dagger] = 0. \quad (\text{B59})$$

The elements of the matrix $\widetilde{\text{U}}$ are given by

$$U_{11} = \left\{ 2 \left[\mu_+ + \left(\frac{\mu_+}{\mu_-} \right)^{1/2} |\mu_0| \right] \right\}^{-1/2}, \quad (\text{B60})$$

$$U_{21} = - \left\{ 2 \left[\mu_+ - \left(\frac{\mu_+}{\mu_-} \right)^{1/2} |\mu_0| \right] \right\}^{-1/2}, \quad (\text{B61})$$

$$U_{12} = \exp[i \arg(\mu_0)] \left\{ 2 \left[\mu_- + \left(\frac{\mu_-}{\mu_+} \right)^{1/2} |\mu_0| \right] \right\}^{-1/2}, \quad (\text{B62})$$

$$U_{22} = \exp[i \arg(\mu_0)] \left\{ 2 \left[\mu_- - \left(\frac{\mu_-}{\mu_+} \right)^{1/2} |\mu_0| \right] \right\}^{-1/2}, \quad (\text{B63})$$

where

$$\mu_+ = |A'_{11}|^2 + |A'_{12}|^2 + |A''_{11}|^2 + |A''_{12}|^2, \quad (\text{B64})$$

$$\mu_- = |A'_{21}|^2 + |A'_{22}|^2 + |A''_{21}|^2 + |A''_{22}|^2, \quad (\text{B65})$$

$$\mu_0 = A'_{11}A'_{21}^* + A'_{12}A'_{22}^* + A''_{11}A''_{21}^* + A''_{12}A''_{22}^*. \quad (\text{B66})$$

Identifying the inverse of $\widetilde{\text{U}}$ with $\widetilde{\text{A}}^{(N-2)}$,

$$\widetilde{\text{A}}^{(N-2)} = \widetilde{\text{U}}^{-1}, \quad (\text{B67})$$

Eq. (B53) [together with Eq. (B57)] is the desired result (44). From the structure of the Green function [cf. Eqs. (25)–(28)] it is clear that the input operators $\hat{a}_{1+}(x, \omega)$ and $\hat{a}_{N-}(x, \omega)$, respectively, can always be written in the form given in Eqs. (B1) and (B2) [with arbitrary N ($N \geq 3$) in place of $N=3$]. With regard to the basic-field operators $\hat{f}(x, \omega)$, both the input operators and the noise operators $\hat{g}_\pm^{(N-2)}(\omega)$ refer to different space intervals. Hence all the commutation relations (45)–(50) are satisfied for arbitrary

N ($N \geq 3$), which implies that the commutation relations (B24)–(B26) remain also valid when $\hat{a}_{N+}(x, \omega)$, $\hat{a}_{N+}^\dagger(x', \omega)$ and $\tilde{\mathbf{T}}^{(N-2)}, \tilde{\mathbf{A}}^{(N-2)}$ are substituted for $\hat{a}_{3+}(x, \omega)$, $\hat{a}_{3+}^\dagger(x', \omega)$ and $\tilde{\mathbf{T}}^{(1)}, \tilde{\mathbf{A}}^{(1)}$, respectively. We finally mention that in a way similar to that outlined above for the input-output relations the extension of the relations (B27) and (B28) to arbitrary N ($N \geq 3$) may be proved correct.

APPENDIX C: OUTGOING-RADIATION CORRELATION FUNCTIONS

When the dielectric plate is in thermal equilibrium the density operator of the matter excitations may be given by

$$\rho_{\text{DP}} = \exp \left\{ - \sum_{i=1}^2 \int_0^\infty d\omega \left(\ln[1 + n_{\text{th}}(\omega)] + \frac{\hbar\omega}{k_B T} \hat{g}_i^\dagger(\omega) \hat{g}_i(\omega) \right) \right\}, \quad (\text{C1})$$

with $n_{\text{th}}(\omega)$ from Eq. (74). Note that this density operator of course corresponds to the thermal-equilibrium state of the basic field $\hat{f}(x, \omega)$ inside the plate. The correlation functions (67) are then calculated to be

$$\underline{\Gamma}_{\{i_\mu\}}^{(p,q)}(\{\omega_\mu\}) = \delta_{pq} \prod_{\zeta=1}^p \delta_{i_\zeta i_{\zeta+p}} n_{\text{th}}(\omega_\zeta) \delta(\omega_\zeta - \omega_{\zeta+p}), \quad (\text{C2})$$

where the set of indices ζ denotes a permutation of the set of indices μ , so that $\omega_{\zeta-1} < \omega_\zeta$ for $2 \leq \zeta \leq p$ or $p+2 \leq \zeta \leq p+q$ [note that $\underline{\Gamma}_{\{i_\mu\}}^{(p,q)}(\{\omega_\mu\})$ vanishes if for any ζ with $p \geq \zeta \geq 2$ the relation $\omega_{\zeta-1} = \omega_\zeta$ is fulfilled].

We now appropriately label the terms that (after disentangling) occur on the right-hand side of Eq. (65). For this purpose we introduce the set $S^{(m,n)}$ of arrangements of the $m+n$ indices ζ (disposed in ascending order) by assigning them to two classes ($K=1,2$) and four (possibly empty) groups ($j=1,2,3,4$). The class indices $K=1$ and $K=2$ refer to the creation and destruction operators, respectively, and the group indices $j=1,2,3,4$ are used to distinguish between the four excitations to be considered. For $K=1$ (2) the indices refer for $j=1$ to \hat{a}_1^\dagger (\hat{a}_1), for $j=2$ to \hat{a}_2^\dagger (\hat{a}_2), for $j=3$ to \hat{g}_1^\dagger (\hat{g}_1), and for $j=4$ to \hat{g}_2^\dagger (\hat{g}_2). The λ_j^K indices of the K th class and j th group are denoted by $\zeta_j^K(i)$, $i=1, \dots, \lambda_j^K$. From Eq. (65) we then find that

$$\begin{aligned} \underline{C}'_{\{i_\mu\}}^{(m,n)}(\{\omega_\mu\}) &= \sum_{S^{(m,n)}} \underline{C}_{\{i_\zeta; i_{\zeta_2}\}}^{(\lambda_1^1, \lambda_1^2; \lambda_2^1, \lambda_2^2)}(\{\omega_{\zeta_1}; \omega_{\zeta_2}\}) \underline{\Gamma}_{\{i_{\zeta_3}\}}^{(\lambda_3^1, \lambda_3^2)}(\{\omega_{\zeta_3}\}) \underline{\Gamma}_{\{i_{\zeta_4}\}}^{(\lambda_4^1, \lambda_4^2)}(\{\omega_{\zeta_4}\}) \\ &\times \prod_{\alpha=1}^{\lambda_1^1} \prod_{\beta=1}^{\lambda_2^1} \prod_{\gamma=1}^{\lambda_1^2} \prod_{\eta=1}^{\lambda_2^2} T_{i_{\zeta_1^1(\alpha)}}^*(\omega_{\zeta_1^1(\alpha)}) T_{i_{\zeta_2^1(\beta)}}^*(\omega_{\zeta_2^1(\beta)}) T_{i_{\zeta_1^2(\gamma)}}(\omega_{\zeta_1^2(\gamma)}) T_{i_{\zeta_2^2(\eta)}}(\omega_{\zeta_2^2(\eta)}) \\ &\times \prod_{\phi=1}^{\lambda_3^1} |A_{i_{\zeta_3^1(\phi)}}(\omega_{\zeta_3^1(\phi)})|^2 \prod_{\chi=1}^{\lambda_4^1} |A_{i_{\zeta_4^1(\chi)}}(\omega_{\zeta_4^1(\chi)})|^2, \end{aligned} \quad (\text{C3})$$

where

$$\underline{C}_{\{i_{\zeta_1}; i_{\zeta_2}\}}^{(\lambda_1^1, \lambda_1^2; \lambda_2^1, \lambda_2^2)}(\{\omega_{\zeta_1}; \omega_{\zeta_2}\}) = \left\langle \left[\prod_{\alpha=1}^{\lambda_1^1} \hat{a}_1^\dagger(\omega_{\zeta_1^1(\alpha)}) \right] \left[\prod_{\beta=1}^{\lambda_2^1} \hat{a}_2^\dagger(\omega_{\zeta_2^1(\beta)}) \right] \left[\prod_{\gamma=1}^{\lambda_1^2} \hat{a}_1(\omega_{\zeta_1^2(\gamma)}) \right] \left[\prod_{\eta=1}^{\lambda_2^2} \hat{a}_2(\omega_{\zeta_2^2(\eta)}) \right] \right\rangle \quad (\text{C4})$$

(the notation ζ_j is used to indicate sets of indices, without distinguishing between the two classes).

-
- [1] L. Knöll, W. Vogel, and D.-G. Welsch, Phys. Rev. A **36**, 3803 (1987).
[2] R.J. Glauber and M. Lewenstein, Phys. Rev. A **43**, 467 (1991).
[3] H. Khosravi and R. Loudon, Proc. R. Soc. London Ser. A **433**, 337 (1991); **436**, 373 (1992).
[4] W. Vogel and D.-G. Welsch, *Lectures on Quantum Optics* (Akademie Verlag, Berlin, 1994).
[5] L. Knöll, W. Vogel, and D.-G. Welsch, Phys. Rev. A **42**, 503 (1990); J. Opt. Soc. Am. B **3**, 1315 (1986).
[6] L. Allen and S. Stenholm, Opt. Commun. **93**, 253 (1992).
[7] L. Knöll, W. Vogel, and D.-G. Welsch, Phys. Rev. A **43**, 543 (1991).
[8] L. Knöll and D.-G. Welsch, Prog. Quantum Electron. **16**, 135 (1992).
[9] M. Fleischhauer and M. Schubert, J. Mod. Opt. **38**, 677 (1991).
[10] G.S. Agarwal, Phys. Rev. A **11**, 230 (1975).
[11] B. Huttner and S.M. Barnett, Europhys. Lett. **18**, 487 (1992); Phys. Rev. A **46**, 4306 (1992).
[12] L. Knöll and U. Leonhardt, J. Mod. Opt. **39**, 1253 (1992).
[13] D. Kupiszewska, Phys. Rev. A **46**, 2286 (1992).
[14] S.-T. Ho and P. Kumar, J. Opt. Soc. Am. B **10**, 1620 (1993).
[15] J.R. Jeffers, N. Imoto, and R. Loudon, Phys. Rev. A **47**, 3346 (1993).
[16] T. Gruner and D.-G. Welsch, Phys. Rev. A **51**, 3246 (1995).

- [17] S.M. Barnett, R. Matloob, and R. Loudon, *J. Mod. Opt.* **42**, 1165 (1995).
- [18] T. Gruner and D.-G. Welsch, *Phys. Rev. A* **53**, 1818 (1996).
- [19] C.W. Gardiner and M.J. Collett, *Phys. Rev. A* **31**, 3761 (1985).
- [20] B. Yurke, S.L. McCall, and J.R. Klauder, *Phys. Rev. A* **33**, 4033 (1986).
- [21] R.A. Campos, B.E.A. Saleh, and M.C. Teich, *Phys. Rev. A* **40**, 1371 (1989).
- [22] D.N. Klyshko, *Phys. Lett. A* **137**, 334 (1989).
- [23] E. Yablonovitch and K.M. Leung, *Physica B* **175**, 81 (1991).
- [24] R.Y. Chiao, P.G. Kwiat, and A.M. Steinberg, *Quantum Semi-class. Opt.* **7**, 259 (1995).
- [25] A.M. Steinberg and R.Y. Chiao, *Phys. Rev. A* **51**, 3525 (1995).
- [26] Ch. Spielmann, R. Szipöcs, A. Stingl, and F. Krausz, *Phys. Rev. Lett.* **73**, 2308 (1994).
- [27] *Amazing Light: A Volume in Honor of the 80th Birthday of Charles Hand Townes*, edited by R.Y. Chiao (Springer, New York, 1996).
- [28] M. Born and E. Wolf, *Principles of Optics* (Pergamon Press, London, 1959).
- [29] Extrapolated from H.R. Philipp, *EMIS Datareview Series* (INSPEC, London, 1987).
- [30] W.H. Louisell, *Quantum Statistical Properties of Radiation* (Wiley, New York, 1990).
- [31] O.W. Greenberg, *Ann. Phys. (N.Y.)* **16**, 158 (1961).
- [32] P.A. Henning, *Phys. Rep.* **253**, 235 (1995).